Cement and Concrete Research 41 (2011) 1257–1278

Contents lists available at ScienceDirect

Cement and Concrete Research

journal homepage: http://ees.elsevier.com/CEMCON/default.asp

Modeling and simulation of cement hydration kinetics and microstructure development

Jeffrey J. Thomas [a,*], Joseph J. Biernacki [b], Jeffrey W. Bullard [c], Shashank Bishnoi [d], Jorge S. Dolado [e], George W. Scherer [f], Andreas Luttge [g]

[a] Schlumberger-Doll Research, Cambridge, MA 02139, USA
[b] Department of Chemical Engineering, Tennessee Tech University, Cookeville, TN, USA
[c] Materials and Construction Research Division, National Institute of Standards and Technology, Gaithersburg, MD, USA
[d] Department of Civil Engineering, Indian Institute of Technology Delhi, New Delhi, India
[e] Center for Nanomaterials Application in Construction, LABEIN-Tecnalia, Bilbao, Spain
[f] Department of Civil and Environmental Engineering, Princeton University, Princeton, NJ, USA
[g] Department of Chemistry, Rice University, Houston, TX, USA

ARTICLE INFO

Article history:
Received 24 June 2010
Accepted 7 October 2010

Keywords:
Hydration (A)
Kinetics (A)
Microstructure (B)
Modeling (E)

ABSTRACT

Efforts to model and simulate the highly complex cement hydration process over the past 40 years are reviewed, covering different modeling approaches such as single particle models, mathematical nucleation and growth models, and vector and lattice-based approaches to simulating microstructure development. Particular attention is given to promising developments that have taken place in the past few years. Recent applications of molecular-scale simulation methods to understanding the structure and formation of calcium–silicate–hydrate phases, and to understanding the process of dissolution of cement minerals in water are also discussed, as these topics are highly relevant to the future development of more complete and fundamental hydration models.

Contents

* Corresponding author.
E-mail address: jthomas39@slb.com (J.J. Thomas).

0008-8846/$ – see front matter © 2011 Elsevier Ltd. All rights reserved.
doi:10.1016/j.cemconres.2010.10.004

1. Introduction

This review endeavors to summarize the past 40 years or so of progress towards the development of mathematical models and simulations for understanding and predicting cement hydration kinetics and microstructure development. A complete and accurate hydration simulation would enable materials engineers not only to predict the performance of concrete in the field, but also to troubleshoot performance problems and even to help design new cementitious materials. Despite significant effort and progress, the ability to perform such a complete simulation has not yet been developed, mainly because cement hydration is one of the more complex phenomena in engineering science. The mechanisms of cement hydration are reviewed in this issue [1]. Portland cement as we know it was invented nearly 200 years ago, but the processes that govern its reaction with water are still a matter of considerable debate, and several different theories are available for describing various aspects of hydration. A number of mathematical constructs have been developed to mimic hydration behavior, but these have generally focused on capturing changes in either select microscopic features or in the overall extent of hydration. Nevertheless, steady progress is being made toward a more comprehensive description of hydration that describes both the development of microstructure and the kinetics.

Mathematical constructs that mimic physical phenomena take a number of forms. In engineering science, these constructs are typically called “models” or “simulations.” To frame the discussion, it is useful to draw a distinction between these terms at the outset. In keeping with prior definitions, we suggest the distinction proposed by Aris [2] in general and by Garboczi and Bentz [3] for cement and concrete in particular. A *model* is “a theoretical construct, which is made using… mathematical language, that can be used to make quantitative predictions about a material's structure or properties.” In contrast, a *simulation* is defined as “some sort of stored numerical or analytical representation of [a] system… which is then operated on by prescribed algorithms that give numerical results for physical quantities of interest.” In other words, a model is the mathematical framework, the “scientific principles expressed in mathematical language” [3], whereas the simulation is the application of those principles to a computational representation of an object. A simple example is helpful. Hooke's law is a model that relates stress and strain for linear elastic materials, whereas the use of a finite element program to predict the elastic deflections of a steel beam under loading is a simulation. In practice, however, many simulations are referred to as models by their authors, and we will not attempt to maintain this distinction everywhere in this paper.

Modeling and simulation, taken together, comprise a spectrum of activities that enable the researcher or engineer to compare observations with theory, to extract physical parameters from experimental data, and to predict system behaviors. Applied to cement hydration, these activities may range from the initial stages of an investigation wherein simple models might be used to gain insight about the major controlling processes at different stages of hydration, to advanced or mature stages wherein complex simulations may be developed by incorporating as much of the known physics and chemistry as possible to predict complicated phenomena such as setting and autogenous shrinkage under realistic conditions.

In Section 2 of this paper we provide a brief historical review of models and simulations for cement hydration covering the past 40 years or so. This review includes a new generation of models and simulations that are now emerging and generating their own set of controversies and debates. These models are typically based on microscopic or macroscopic principles and generate information at length scales no finer than about 1 μm. Recent results obtained from these new models are discussed in more detail in Section 3. In Section 4, the scope of the paper is expanded to discuss molecular modeling of cement hydration products and *ab initio* calculations of mineral dissolution. Recent results from these areas of research have great potential for improving hydration simulations by providing information on processes occurring at atomic or nanometer length scales. Finally, in Section 5 some immediate and longer-term modeling efforts are suggested that could help answer some key questions about the nature of cement hydration and how it can be controlled more effectively.

A critical component of any modeling or simulation effort is the choice of assumptions that are made to simplify the problem and make it mathematically and computationally tractable. These assumptions endow each particular model with its own set of strengths and limitations that should be acknowledged and considered when applying the model to a particular case. Therefore, in the following sections we will take care to note the assumptions that are invoked in each model.

2. Historical overview of kinetic models

2.1. Single-particle models

Numerous single particle models have been presented in the literature, many of which are discussed in detail in a recent review by Xie and Biernacki [4]. Here, only a pair of models that illustrate the range of possibilities is discussed. In an early and influential review of cement hydration kinetics research published in 1968, Kondo and Ueda [5] discuss a model developed the previous year by Kondo and Kodama [6] that characterized the hydration kinetics of alite using an assumption of concentric layered growth of hydrates of uniform thickness on a single reacting spherical cement particle (see Fig. 1).

To implement this model, Kondo et al. [5,6] also assumed that an initial metastable layer forms upon the first contact of cement with water and acts as a barrier to dissolution, slowing the reaction and leading to the so-called induction period. The layer dissolves or becomes more permeable with time leading to an accelerating rate. As hydration proceeds, the cement particle shrinks and is replaced by a layer of inner hydration product, while from the outside of the barrier layer, an outer layer of hydration product grows outward into the capillary pore space. As the thickness of the product layer around the particles increases, its resistance to diffusion of reactant ions increases,

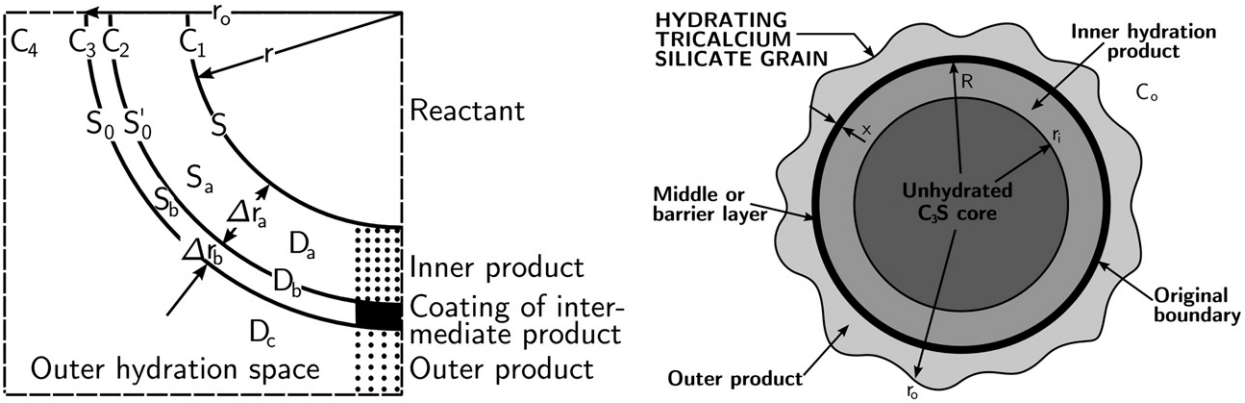

Fig. 1. Schematic representation of a hydrating C_3S grain in concentric growth models by Kondo et al. [5,6] (left) and Pommersheim and Clifton [7] (right).

and the kinetics eventually shifts to a diffusion-controlled regime wherein the rate continuously decelerates. With this model, the rates of the various reaction steps are evaluated separately, and the overall rate of reaction is taken to be that of the slowest step.

In 1979 and 1982, Pommersheim, Clifton, and Frohnsdoff [7,8] presented two papers describing an integrated reaction–diffusion single-particle model for C_3S hydration that utilizes many of the features of the original model of Kondo et al. [5,6] described above, but which is more mathematically rigorous. A schematic of their model is also shown in Fig. 1. Based on a conceptual model for cement microstructure development presented by Williamson in 1972 [9], they went on to propose that hydration might be modeled by what was then already a classical approach for handling reaction and diffusion at phase boundaries. Effectively, they approximated the solution to a time-dependent diffusion equation in spherical coordinates for the transport of water through the growing product layers:

$$\frac{\partial C}{\partial t} = \frac{1}{r^2}\frac{\partial}{\partial r}\left(Dr^2\frac{\partial C}{\partial r}\right) \tag{1}$$

and they solved this equation for the pseudo-steady-state condition $dC/dt = 0$ and the boundary conditions $r = R$, $C = C^o$, $r = r_c$, and $C = C^{eq}$ where r is the radial location within the product layer, R is the original radius of the cement grain (assumed to spherical), C is concentration, the subscript "c" indicates the radius of the unhydrated core, and the superscripts "o" and "eq" are for a fixed value and value at equilibrium respectively.

This equation is solved along with a mass balance constraint applied at the surface of the shrinking core that equates the rate of chemical reaction and the rate of mass diffusion. An advantage of this model is that it allows the seamless integration of a boundary growth reaction that could occur at two surfaces and diffusion through a product layer. Thus, the boundary conditions for this equation would necessarily involve two moving interfaces: that of the shrinking C_3S particle core and that of the growing outer surface of the C–S–H outer product. Williamson's microstructural model [9] characterized C_3S hydration as proceeding via the dissolution of C_3S particles and concomitant precipitation of both inner product C–S–H, which would grow at the interface between the shrinking C_3S particle core and the product layer, and outer product C–S–H, which would grow at the interface between the product layer and the pore solution. As with the model of Kondo et al. [5,6] a metastable layer consisting of a third form of C–S–H was assumed to be present initially as a membrane on the surface of the C_3S particle. In this case, the membrane acts as an interface between the inner and outer product and has unique physical properties of density and diffusivity.

In the Pommersheim and Clifton model [7], the rate of reaction is expressed in terms of the dimensionless radius y:

$$\frac{dy}{dt} = \frac{-1/\tau}{y^2\left[\left(\frac{1}{my^2} + \frac{1}{y} - 1\right) + \frac{D_i}{D_x}\frac{x}{R} + \frac{D_i}{D_o}\left(1 - \frac{R}{r_o}\right)\right]} \tag{2}$$

where $y = r_c/R$, $\tau = aR^2\delta/(C^oD_i)$, ($\delta$ is the density of C_3S, C^o is the concentration of water, and a is a stoichiometric coefficient), the D terms are diffusivities, $m = kR/D_i$ (k is the reaction velocity), x is the thickness of the metastable layer, and the subscripts i, o and x are for the inner, outer and metastable product layers, respectively.

While this model explicitly accounts for growing inner and outer product, it also incorporates numerous simplifying assumptions so that a single tractable differential equation could be obtained. Among the many assumptions are: first order reaction kinetics, water as the transported (diffusing) reagent, coupled growth of the inner and outer product, e.g. the amount of outer product formed depends only upon the amount of inner product formed, the reaction stoichiometry and the molar density of the inner and outer product, and an assumption that makes r_o a simple algebraic function of y, one that would later be used by Jennings and Johnson [10]. The thickness of the metastable barrier layer is modeled empirically as a decaying exponential with no supporting experimental evidence. Also notable, Pommersheim and Clifton proposed that the transport properties of the inner product are constant (constant D_i), yet suggested that D_o decreases with increasing degree of hydration. While this was a progressive idea, it was again implemented using an empirical correlation tied to the overall system porosity rather than the local porosity of the C–S–H surrounding a single particle.

Two general problems with single-particle models of cement are that they do not account for particle–particle interactions such as impinging product layers, and they do not accurately represent the overall kinetics of a collection of hydrating particles with a wide range of sizes [11,12]. The kinetics of polydisperse powders can be modeled approximately by adding the effects of individual particle sizes. When this is done, the fit parameters are different than those obtained by assuming a single averaged particle size [13]. Various models and modeling approaches have been proposed that incorporate effects of particle size distribution [14–17]. Among these is the widely used and cited Knudsen equation [15]. While these relations can provide some insight about the effects of particle size distribution on hydration, their derivation and use tend to be cumbersome.

Some empirical approaches to integrating single-particle models into a more global model of cement hydration have been fairly successful. In 1984, Parrot and Killoh [18] analyzed quantitative X-ray

diffraction (QXRD) data on the hydration of cement pastes with a wide range of portland cement compositions, particle size distributions, and water/cement ratios. For each mix formulation, they extracted from QXRD data the rate of dissolution of each of the four major phases in portland cement clinker. Based on these time-dependent data, they formulated a set of coupled equations to model the dissolution rate of each phase as a function of water–cement mass ratio, relative humidity, and specific surface area of the powder. These equations are essentially modified versions of earlier single-particle models applied to each clinker phase and adjusted to account for global microstructure effects such as water/cement ratio and degree of saturation. Empirical fitting parameters in the equations were determined by interpolation of the X-ray diffraction data. Solving the coupled equations for other mixes, within the range of calibration of the model, provided excellent predictions of the degree of hydration of each clinker phase, the overall bound water content, and heat evolution of the paste. In 1997, Tomosawa [19] proposed a model in the same spirit as that of Parrott and Killoh, also based on a single-particle model but attempting to account for the influence of powder fineness and water/cement ratio on the hydration kinetics. Both the Parrot and Killoh model and the Tomosawa model are quite effective within their sphere of applicability, and they are easy enough to implement that they have been used as the kinetic basis for some more modern approaches to modeling cement hydration and property development [20–22].

While these approaches can successfully predict aspects of cement hydration kinetics, it should be noted that they are both empirical and interpolative in nature. As such, their predictions may be valid only for cement mixes similar to those used to calibrate the fitting parameters, and caution should be used in applying them to mixes outside the range of calibration. One would generally expect that a recalibration of the parameters would be required for new cements or markedly different mix proportions.

As noted earlier, an important limitation of all single particle models is that they do not account for particle–particle interactions and space filling considerations in a hydrating paste. Thus the kinetic effects of impinging product layers from adjacent particles and overall filling of the available pore space are ignored. In this sense, they are clearly distinguished from nucleation and growth models discussed in the next section, which account for decelerating hydration rates by space filling and impingement phenomena rather than diffusion-controlled kinetics.

2.2. Nucleation and growth models

Experimental observations suggest that the rate of formation of C–S–H hydration product is the rate-controlling process of hydration at early ages [23,24]. These observations have led to the development of models of hydration kinetics based on nucleation and growth phenomena. Nucleation and growth, although distinctly different kinetic processes with separate rate constants and driving forces, are often modeled together as a single general process by which one phase transforms into another. Examples of such phase transformations include many solid–solid transformations (such as the austenite-to-pearlite transformation in steel), liquid–solid transformations (such as freezing), and precipitation of solid phases out of a solution. The process is based on the premise that while the final phase has a lower free energy than the initial phase, there is an energy barrier to nucleating the first regions of the transformed phase that is associated with the work required to form the interface between the two phases and any misfitting stresses that arise. This energy barrier can be overcome by random thermal fluctuations occurring either in the bulk (homogeneous nucleation) or at specific energetically favorable sites (heterogeneous nucleation). Once a stable nucleus forms, it will grow as long as the thermodynamic driving force remains in place and there is room for it to grow.

If certain simplifying assumptions are made, the overall kinetics of nucleation and growth can be described mathematically. In the early stages of a nucleation and growth process when the fractional degree of transformation is low, individual regions of growing product do not interfere with each other and a simple power law behavior can be observed. At later times the impingement of adjacent regions of product must be accounted for, and the behavior is more complex. These two situations will be discussed separately below.

2.2.1. Early nucleation and growth

Once a stable nucleus has formed and started to grow, the change in its volume with time will depend on the local conditions and on its morphology. If the reactants required to supply the transformation reaction are continuously replenished so that the level of supersaturation is constant, then the kinetics are described as phase-boundary controlled. In this case the rate of growth of a region in any linear direction will be constant, and its volume will increase with time according to:

$$v \propto (Gt)^p \tag{3}$$

where G is a linear growth rate and p is the number of dimensions in which growth is occurring, $p=1$ for needles, $p=2$ for sheets, and $p=3$ for isotropic growth (i.e. spheres). If the rate at which reactants are supplied to the growing region is the rate-controlling step, then the reaction is diffusion controlled, and the volume of an individual region is given by:

$$v \propto (Gt)^{p/2}. \tag{4}$$

The overall rate of transformation will depend on how the number of nuclei present in the system changes with time. Two limiting cases can be analyzed. If nucleation is initially rapid but then quickly stops due to exhaustion of the available nucleation sites or a reduction in driving force due to depletion of the species required for nucleation, then it is reasonable to approximate that all of the nuclei are present at the start of the reaction, a condition known as site saturation. In this case the total volume of the product phase is simply $V=Nv$, where N is the number of nuclei, until the different regions of hydration product begin to impinge.

If active sites for nucleation within the initial phase are not depleted, then nucleation will not stop abruptly, but will continue at a rate that is proportional to the amount of remaining untransformed material at any given time. This is referred to as continuous nucleation. In this case, the total volume of the transformed phase as a function of time can be calculated by integrating the expression for the volume of an individual region with respect to time, which increases the value of the exponent given in the equations above by one [see e.g. 25].

From these considerations, it can be seen that a power law behavior in time is always predicted for the early stages of the transformation process, such that the overall volume of the final phase, V, will follow [26,27]:

$$V \propto t^m \quad \text{with } m = p/s + q \tag{5}$$

where p is the growth dimensionality as defined above, s is the type of rate control ($s=1$ for phase boundary, $s=2$ for diffusion) and q is the type of nucleation ($q=0$ for site saturation, $q=1$ for continuous nucleation). The values of m that can be obtained range from 1/2 to 4. Note that if an intermediate value of m is measured experimentally the correct interpretation, e.g. values for p, s, and q, may not be clear.

2.2.2. The JMAK nucleation and growth equation

The volume of the transformed phase will only increase with simple power law behavior in the early stages of the process before

adjacent regions of growing product impinge [25]. However, the impingement process can be described mathematically by making assumptions about the distribution of nuclei within the transforming volume. The simplest and most widely used equation, proposed independently by Avrami [26], Johnson and Mehl [28], and Kolmogorov [29], is derived using the assumption that nuclei are randomly distributed everywhere within the transforming volume. The well-known result, known as the Avrami or JMAK equation, is:

$$X(t) = 1-\exp\left[-(kt)^m\right] \quad (6)$$

where $X(t)$ is the volume fraction that has transformed at time t, m is as defined in Eq. (5), and k is a combined rate constant that incorporates the rates of growth and nucleation. Because these rates are temperature dependent, the equation only applies to isothermal systems. This equation has frequently been applied to kinetic data for C_3S hydration, resulting in a wide range of values of the exponent m being reported. Because the value of m is directly related to physical parameters such as the product morphology and rate limiting step (see Eq. (5)), this discrepancy has led to conflicting interpretations regarding the hydration process. As will be discussed, while the mathematical form of the JMAK equation allows it to be fit reasonably well to C_3S hydration kinetics, at least up to the maximum hydration rate, it does not provide a geometrically appropriate representation of the hydration process and thus the fitted parameters have limited physical significance.

Forty years ago, Tenatousse and de Donder [30] were the first to apply the JMAK nucleation and growth equation to C_3S hydration data, in their case obtained by isothermal calorimetry. They reported an exponent value of $m=3$, and by performing fits obtained at different temperatures were able to calculate an activation energy of 33 kJ/mol. This early work reached the important conclusion that nucleation and growth kinetics extend past the maximum in the rate of hydration, which conflicted with the prevailing opinion [31] that the acceleration and initial deceleration periods are mechanistically distinct, with nucleation and growth only controlling the former (a viewpoint that has not entirely disappeared). Brown et al. [27] presented a more detailed mathematical model based on Eq. (6) which for the first time investigated the mechanistic underpinnings of the exponent m for cement hydration. Unfortunately, their reanalysis of quantitative X-ray diffraction data originally published by Kondo and Ueda [5] resulted in a very low value of $m=1$, which led them to unphysical conclusions regarding the hydration process. Similar values of m close to unity were reported more recently from analysis of kinetic data obtained from measurements of the pore structure development by repeated freezing of the paste [32,33]. In the latter case, the freezing process itself may have interfered with the kinetics by damaging the gel [34]. Other researchers have measured values of m between 2 and 3, using isothermal calorimetry [35,36], quasielastic scattering [37–39], and small-angle X-ray scattering [40].

In an important review of hydration mechanisms published in 1989, Gartner and Gaidis [41] pointed out for the first time that the assumption of spatially random nucleation used to derive the JMAK equation was dubious for cement hydration due to its heterogeneous particulate nature. This point was not stressed, however, and the JMAK equation continued to be widely used. In 1999, Thomas and Jennings [36] showed that the JMAK equation could be used to accurately fit the calorimetry rate curve for C_3S to a point partway along the downslope of the rate peak (see Fig. 2), at which point the fits inevitably diverged. They observed that the value of the exponent m obtained depended on how far past the rate peak the fit was extended, and they concluded that for their experimental data accurate fits were obtained if the fits were extended to the point where the rate had fallen to 70% of its maximum value. When this was done, the values of m obtained were always close to 2.65. This value has no particular significance in itself, but it was subsequently used as a convenient fixed value of m for fitting the JMAK equation to QENS data for C_3S hydration [42–44], since the precision of the kinetic data obtained from that technique does not permit an independent determination of m.

In a review of the cement hydration process published in 2002, Gartner et al. [45] reiterated that the value of m decreased as the range of data that was being fitted extended out farther in time, and he made the important observation that when only the early data (the first several hours of accelerating hydration rate leading up toward the rate peak) are considered, the value of m is well over 3. Thomas [46] later showed that when the JMAK equation is applied to calorimetry rate data only up to the rate peak, the value of the exponent is about 3.74 (see Fig. 2, at right). Since the geometric impingement issues associated with this type of process begin to affect the kinetics even before the rate peak, it is reasonable to assume that for C_3S hydration m is close to 4, its theoretical maximum value. Eq. (6) indicates that this value can only be obtained with phase boundary rate control, three dimensional growth, and continuous nucleation. Note that since the nucleation rate is proportional to the amount of untransformed material remaining where new nucleation sites can form, the overall nucleation rate in the system always decreases with time.

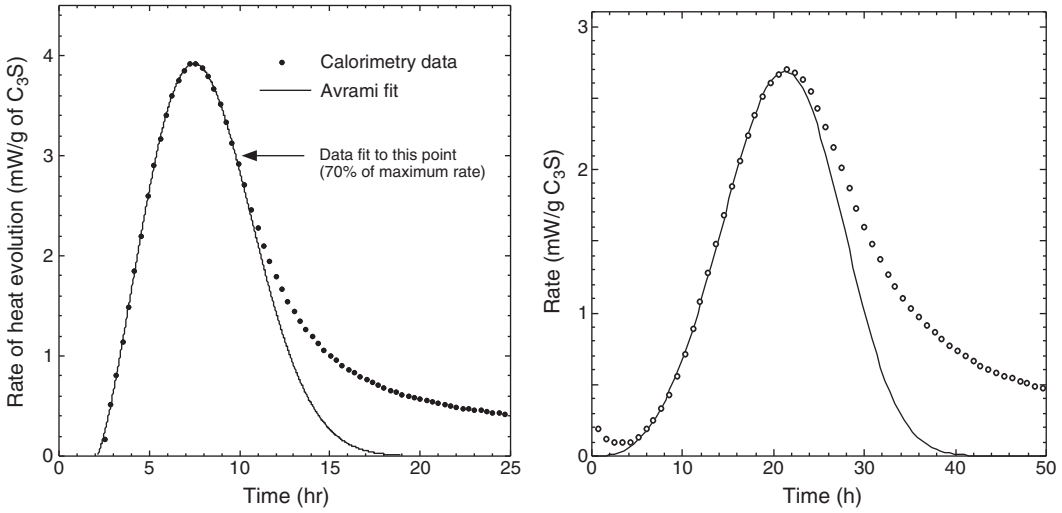

Fig. 2. Application of the JMAK nucleation and growth equation to isothermal calorimetry data for C_3S hydration. Left: the upslope and peak region can be fit accurately, resulting in a fitted value of exponent m close to 2.65 (after [36]). Right: if the JMAK fit is applied only to data up to the peak, a higher value of $m=3.74$ is obtained (after [46]). See text for discussion of the significance of this difference.

It is clear from experimental evidence, particularly microscopy conducted during the first several hours of hydration, that nucleation of the cement hydration products occurs primarily on the surface of the cement grains. This is implicitly assumed by all single particle models, which model concentric growth inward and outward from the particle surface. However, confining nucleation to the particle surfaces violates the assumption of random nucleation throughout the transforming volume that is used to derive the JMAK equation, limiting its utility for modeling the hydration kinetics. Two major implications of this problem are that the fitted values of the rate constant cannot be translated into useful physical parameters, such as the growth rate and nucleation rate, and that the JMAK equation cannot account for the important effect of particle size, or more precisely the specific surface area of the cement, on the hydration kinetics.

2.2.3. A numerical model for nucleation and growth on a planar surface

To better understand their experimental data on the rate of hydration of C_3S in controlled dilute lime solutions of different concentrations, Garrault and Nonat [47] developed a numerical model to simulate the growth of C–S–H nuclei on the surface of C_3S. In this model, nuclei of C–S–H form on a single planar surface. At each step in the simulation, the nuclei grow both parallel and perpendicular to the surface. They found that good fits to their experimental data were obtained if the perpendicular growth rate is assumed to be higher than the parallel growth rate. It is not clear whether this would also be the case in a paste specimen. This model predicts that in the initial stages of hydration the surface of the particles is only partially covered by hydrates, with a complete layer forming only after the peak of hydration. While this model accounts for the fact that nucleation of hydration product occurs primarily on the surface of the hydrating grains (the main problem with application of the JMAK equation), it does not account for interactions between product layers arising from different particles (impingement), which is important in a paste specimen.

2.2.4. The mathematical boundary nucleation and growth model

In 2007, Thomas [46] pointed out that an existing but little-known mathematical formulation derived to describe a solid–solid phase transformation in a polycrystalline material that is nucleated preferentially on grain boundaries provides a better geometric analogy to the cement hydration process than does the JMAK equation. In this case, the surface of the cement or C_3S particles is analogous to the grain boundaries where nucleation occurs, and the fluid-filled pore spaces between the particles are analogous to the grains themselves. This boundary nucleation and growth (BNG) model, originally published in 1956 by Cahn [48], assumes that nuclei form only on planar boundaries that are randomly oriented and distributed within the volume. Cahn's derivation assumed a constant nucleation rate per unit area of untransformed boundary (a form of continuous nucleation) and a constant growth rate of the nucleated regions in all linear directions. While derivations based on other assumptions are possible, these assumptions fortuitously correspond to the value of $m=4$ measured for the early C_3S hydration process (see above).

The BNG formulation is:

$$X = 1-\exp\left[-2O_v^B \int_0^{G_t} \left(1-\exp\left(-Y^e\right)\right)\right] \tag{7}$$

where

$$Y^e = \frac{\pi I_B}{3} G^2 t^3 \left[1-\frac{3y^2}{G^2t^2}+\frac{2y^3}{G^3t^3}\right] (\text{for } t > y/G)$$

$$Y^e = 0 \ (\text{for } t < y/G)$$

where G is the linear growth rate, I_B is the nucleation rate per unit area of untransformed boundary, and O_v^B is the total boundary area per unit volume. The fraction of the boundary area that is covered with the transformed phase is given by $Y=1-\exp(-Y^e)$. Evaluation of the BNG equations is done numerically, and temporary variables Y^e and y disappear during the integration to find X.

Thomas [46] noted that the three physical parameters in the BNG model (G, I_B, and O_v^B) are codependent with only two degrees of freedom, and he proposed two rate constants, each with units of inverse time:

$$k_B = \left(I_B O_v^B\right)^{1/4} G^{3/4} \tag{8}$$

$$k_G = O_v^B G. \tag{9}$$

The dimensionless ratio k_B/k_G is an important physical parameter. When $k_B \gg k_G$, then the internal boundaries become densely populated with nuclei and a continuous layer of hydration product forms on the boundaries early in the overall process, shutting off further nucleation. The remainder of the transformation occurs by a relatively slow process of thickening of the product layers. The resulting rate of transformation with time dX/dt is an asymmetric peak with a more gradual downslope (see fits in Fig. 3). If $k_G \gg k_B$ then the boundaries are sparsely populated with nuclei such that they are effectively randomly distributed in the volume, and the BNG model reduces to the JMAK equation, which produces a nearly symmetric dX/dt peak (see fits in Fig. 2).

When applied to calorimetry data for pure C_3S or alite powder, the BNG model provides a noticeably better fit than does the JMAK equation (see Fig. 3). Instead of deviating from the data early on the downslope, the entire early rate peak is accurately fit. However, the fits continue to deviate from the post-peak data. The values of k_B/k_G obtained were close to 1, indicating behavior intermediate between the two extreme cases noted above. The BNG model has also been applied with success to C_3S hydration data obtained by QENS [49]. Interestingly, Thomas et al. [50] recently found that calorimetry data for $CaCl_2$-accelerated C_3S paste could be fit quite accurately out to a high degree of hydration, with no apparent point of deviation between the model and the fit (Fig. 3, at right). This is discussed further in Section 3.2.

2.2.5. Limitations of nucleation and growth modeling

Nucleation and growth models for hydration of cement are being applied with increasing sophistication, and some recent results obtained from the BNG model are discussed further in Section 3. Here we note, however, that such models must be used with caution. As discussed above, while the conventional JMAK model has been used for many years and in many cases provides reasonable fits to kinetic data, the serious mismatch between its assumption of random volume nucleation and the observation that C–S–H nucleates on mineral surfaces means that the parameters from such fits will have little or no physical meaning.

The boundary nucleation model is a more realistic model for hydration, and it provides fits that range from moderately to significantly better, as compared to the JMAK model (see Fig. 3). However, even when the assumed mechanisms for nucleation and growth are valid for a given mineral, the boundary nucleation model is only approximate, because it assumes that the boundaries are static. In fact, dissolution causes the reacting boundaries to move, and the development of hydration products on either side of the original interface (i.e., away from and into the reacting grain) will be different.

The extension of the boundary nucleation model to cement paste containing multiple hydrating minerals also presents serious challenges. During stages 2 and 3, the hydration of C_3S is predominant, so the other phases can be assumed to be relatively inert, but this is not

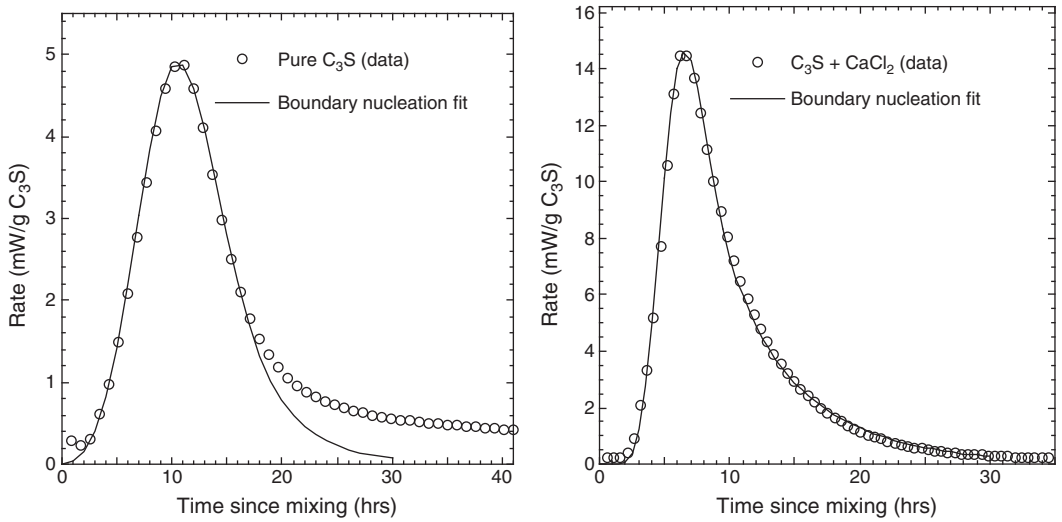

Fig. 3. Application of the boundary nucleation and growth (BNG) model to isothermal calorimetry data for hydration of (a) pure C_3S and (b) $CaCl_2$-accelerated C_3S, after [50].

true beyond the peak rate of stage 3, where hydration of C_2S becomes significant. To model this period, it would be necessary to invoke a second transformation rate. As a mathematical convenience, it is tempting to add together two different boundary nucleation functions, but it is not clear that they are independent. For example, while the nucleation of C–S–H from hydration of C_3S apparently occurs on the surface of the cement grain, the products from subsequent hydration of C_2S might form within the existing mass of C–S–H, rather than on the boundary. During hydration of pure C_2S, the product would probably grow from the boundary, so the behavior of C_2S in the cement might be qualitatively different from that of the pure material. Even if the appropriate functions for fitting were known, the number of parameters needed to describe concurrent hydration of multiple phases would be too large to permit an unambiguous fit, without independent information about the progress of the reaction. Therefore, it becomes impractical to interpret changes in the parameters with reaction conditions when more than one phase is reacting.

In spite of these concerns, the boundary nucleation model seems to capture the progress of reaction of C_3S and some types of cement (i.e. those whose early hydration is dominated by C_3S) to well past the maximum hydration rate. In a recent study, the BNG model was used successfully to analyze the hydration kinetics of cement pastes subjected to various ramps in temperature and pressure [51].

For the version of the BNG model used to date, the nucleation rate per unit area of exposed particle surface is assumed to be constant. In this case, the absolute nucleation rate is highest just after mixing, and then declines gradually as the surfaces become covered with product. However, according to nucleation theory, the nucleation rate should also depend on the degree of supersaturation of the pore solution with respect to hydration product. Recent simulations of C_3S hydration by Bullard [52] indicate that nucleation is confined to a short interval just after mixing when the supersaturation is highest; this lowers the supersaturation and subsequent hydration occurs by a process of pure growth. Interestingly, the mathematical BNG model can be modified to simulate this situation by having growth occur from a fixed number of nuclei that are already present at time $t=0$ [53], a condition known as site saturation. The difference in the model behavior with these two assumptions is primarily in the very early stages, with the site saturation assumption giving a shorter apparent induction period than the continuous nucleation assumption. When fitting chemical shrinkage data for cement, the site saturation assumption appears to provide slightly better fits than the continuous nucleation assumption, at least for $T \leq 40$ °C [53].

Although the BNG model derived by Cahn [48] accounts for the location of the nuclei, it does not allow for impingement of the product phase by an untransformed boundary, because experiments on transformations of metals showed that precipitates could grow across grain boundaries. However, this is not the case for hydration, where the products cannot penetrate the neighboring unhydrated grains, but will stop at the surface (or, proceed into the grain at a greatly reduced rate). Johnson and Mehl [28] developed an alternative model, in which nuclei formed on the inner surface of a sphere grow into the sphere, but cannot pass through the surface to transform adjacent regions. Models for growth constrained by impenetrable boundaries can be analyzed using the "time cone" or "causal cone" method introduced by Cahn [54]. That approach has recently been generalized by Villa and Rios [55], who provide equations for precipitation within polyhedral, cylindrical, spherical, or planar boundaries, with constant or time-dependent growth and nucleation rates, or from a constant number of nuclei. A model with impenetrable boundaries may be more appropriate for hydration than the version by Cahn, although in practice, if the nucleation rate is high such that the boundaries transform before being reached by adjacent product regions, the distinction will not matter.

While it is not yet clear which specific assumptions are most accurate for cement hydration, the ability to modify nucleation and growth models to match the findings of numerical simulations and microscopic investigations makes them useful as tools for investigating the actual mechanisms at work during early hydration. For example, mixing energy is known to have an effect on hydration kinetics. The setting point shifts by several hours for the same cement paste, according to whether it is mixed by hand or in a blender. While the mechanism for this effect is not known, one reasonable hypothesis is that intense mixing causes physical disruption of the hydration layer, thus changing the nucleation rate. This hypothesis could be tested by investigating changes to the boundary nucleation and growth parameters with mixing energy.

2.3. Hydration simulation models

From the discussion in Sections 2.1 and 2.2, it should be clear that relatively simple models such as single-particle and nucleation and growth models can at best accurately reflect the hydration of a paste during a limited period of time when the temperature is constant, and that, in their present form, these models provide no way to simulate such phenomena as strength development, porosity, and the heterogeneous distribution of multiple cement phases. To accurately simulate the complex hydration process of a cement paste requires a more comprehensive approach that simultaneously accounts for multiple physical phenomena. The need for a true microstructural simulation

platform for cement was anticipated in 1968 by Frohnsdorff et al. [56], but lack of computing power left no way of implementing such a model for at least the next 20 years.

In theory, a complete hydration simulation should accurately simulate the hydration kinetics as well as the microstructure development, since the same fundamental processes underlie both. In practice, the many assumptions and simplifications required to address such a complex problem as cement hydration means that most models tend to be better at some aspects of the hydration process than others. In this context, it should be noted that some of the models discussed in this section were designed to simulate microstructure development, and provide only an approximation of the hydration kinetics, particularly at early times.

2.3.1. The Jennings + Johnson microstructure simulation model

In 1986, Jennings and Johnson [57] published the first microstructure simulation model, marking the start of a new era in cement modeling. The model attempted to reflect the complex distributed nature of the particulate cementitious system with the ultimate goal of producing a platform without preconceived and possibly artificial assumptions that were necessarily used in prior models to average the ensemble behavior. The cement particles were represented as spheres placed inside a cubic volume of paste, and hydration was simulated as the reduction in the radii of the anhydrous phases and the concentric growth of C–S–H layers on the surface of these particles, similar to the single-particle models described earlier (see Fig. 4). However, this new model could account for many additional complexities, such as particle size and particle size distribution, the location and number of calcium hydroxide nuclei, volume changes associated with dissolution of anhydrous phases and precipitation of product phases, and the distribution of phases when growing product layers collide.

The heart of the Jennings and Johnson simulation platform is a three-dimensional microstructure that evolves with time. The spherical particles are represented by the coordinates of their centers and radii, and overlaps between particles (impingement) are accounted for by redistribution of products in space. Calcium hydroxide particles grow from new nuclei in the pore space. The approach of representing shapes using properties that are not discretized onto a grid has a long history in computational physics where it is referred to as an "off-lattice" approach [58]. In its adaptation to represent cement particles and hydration products, however, the off-lattice representation has recently been called the "vector" approach to cement hydration [59].

In the final analysis, Jennings and Johnson developed a rather detailed framework for a type of simulation that could incorporate mechanistic aspects of cement hydration, but the implementation was limited. For example, rigorous kinetic and transport effects or even a suitable algorithm for solving the relevant differential equations that would arise from solution phase and particle material balances and transport effects were not included in the model. Likewise, pore solution chemistry, C–S–H nucleation, and other important mechanistic aspects of hydration were suggested, but not demonstrated. Though the simulation could accommodate kinetics, rate expressions were not explicitly incorporated within the software infrastructure. Due to limited computational power at the time of development, this model was not widely used and could not be developed further. However, it paved the way for other microstructural simulations that would follow, particularly HYMOSTRUC [60] (discussed next) and CEMHYD3D [61] (discussed in Section 2.3.3).

2.3.2. The HymoStruc model

Using a vector approach similar to that pioneered by Jennings and Johnson [57], van Breugel [61,62] developed a similar microstructure simulation model that he called HYMOSTRUC, an acronym for HYdration, MOrphology, and STRUCtural development. Like Jennings and Johnson, van Breugel utilized a 3-D virtual microstructure consisting of equally spaced spherical particles, though he chose to populate his microstructure with particle sizes that followed a Rosin–Rammler model. As the particles react, concentric layers of hydrates form around cement grains causing particles to grow and come into contact with each other (see Fig. 5). Only a single hydration product is assumed to form. As with the Jennings and Johnson model, HYMOSTRUC uses various mass and volume balance rules to accommodate microstructural changes due to dissolution and precipitation of various phases. The model treats the entire microstructure in only a statistical fashion, rather than following the hydration of each individual particle. This approach allows the model to be computationally tractable, but localized information regarding, for example, pores and connectivity is not calculated and thus the approach is not well suited to model the evolution of cement microstructure.

At the heart of HYMOSTRUC is the following equation that relates the extent of reaction $\alpha_{x,t}$ at any time t, for particle x, and the

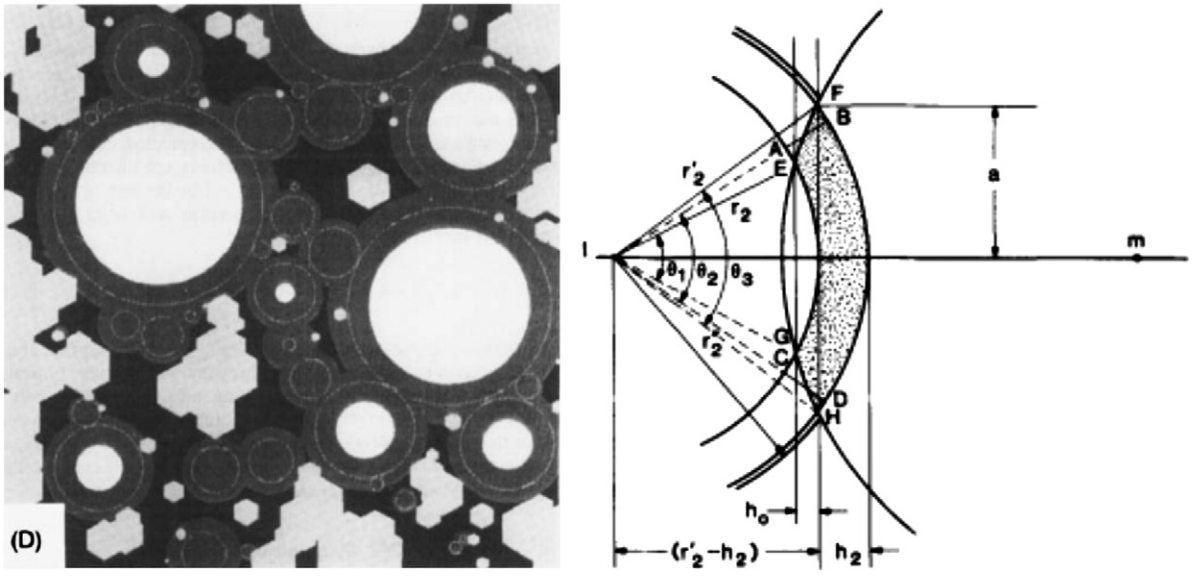

Fig. 4. Microstructure (left) and adjusting for overlaps (right) in the Jennings and Johnson hydration simulation model [57].

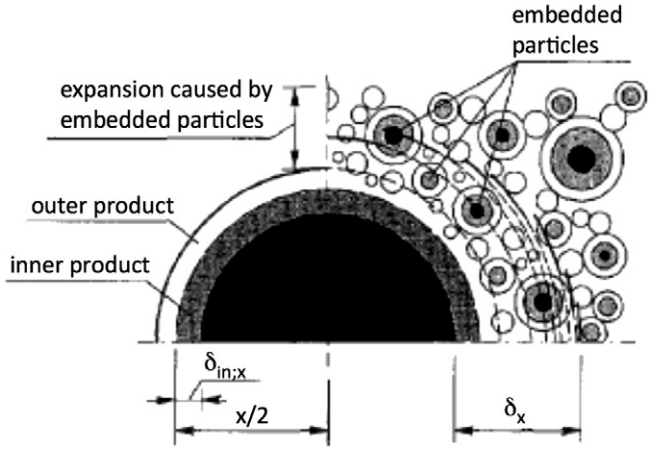

Fig. 5. Schematic of hydration in the HYMOSTRUC microstructure model [106]; the hydration is simulated as the concentric growth of particles.

incremental amount of dissolution tracked in terms of penetration depth, $\delta_{in;x,j}$:

$$\delta_{in;x,j} = \frac{x}{2}\left[1-\left(1-\alpha_{x,j}\right)^{1/3}\right] \tag{10}$$

where $\delta_{in;x,j} = R - r$, where R is the original particle radius and r is the radius of the partially dissolved particle at time t. To link microstructural changes to time and temperature, van Breugel devised an elaborate finite difference model that contains kinetic-like terms:

$$\frac{\Delta\delta_{in;x,j+1}}{\Delta t_{j+1}} = K_o(.)\Omega_1(.)\Omega_2(.)\Omega_3(.)F_1(.)\left[F_2(.)\left(\frac{\delta_{tr}}{\delta_{x,j}}\right)^{\beta_1}\right]^{\lambda} \tag{11}$$

where j is an integer that identifies the simulation time interval, $K_o(.)$ is a rate factor, the Ω terms link water-related microstructural changes to the rate of cement particle conversion, the F terms are the temperature dependencies, δ_{tr} is a penetration thickness that triggers transition to a diffusion controlled behavior, β_1 is an empirical exponent, and $\lambda = 1$ for $\delta_{x,t} >= \delta_{tr}$ and zero for $\delta_{x,t} < \delta_{tr}$. While F_1 takes on an Arrhenius form, it contains a strictly empirical correlation for the activation energy as a function of cement composition. Similarly, while logical, the F_2, the Ω terms, and the transition thickness are all empirical expressions based on large experimental datasets and regression analysis. Such models are not fundamentally based and will require extensive recalibration for systems that are outside the database.

Like the Jennings and Johnson model, HYMOSTRUC does not account for solution phase chemistry or real transport phenomena, nor does it incorporate suitable solution methodologies to support the differential equations that would arise. The authors of this model noted that if the hydration of every individual particle in the model were to be followed the computation would become too large and time-consuming to be carried out. So, only a statistical approach to reaction rates is used, assuming that the reaction rate of each particle depends only on its size. Since this model does not calculate interactions or overlaps between particles, the microstructure information is not utilized in the simulations and the state at any step in the calculation can theoretically be calculated directly from the initial state, possibly using only semi-empirical equations and without using the microstructure information available in the model.

The HYMOSTRUC model was later modified to account for random packing of particles replacing the original assumption of equal spacing between the particles [63]. In this extended version of the model, the pore-structure constant was determined by analysis of two-dimensional slices from the simulations. At the same time, the model was extended for calculating autogenous shrinkage based on the pore structure, using a combination of various empirical equations fitted with pore-parameters calculated from the model. The specifics of how these parameters were extracted from the model are not clear. Another pixel-based method to analyze pores was later added to the model [64].

2.3.3. The CEMHYD3D digital hydration model

CEMHYD3D is a 3D microstructure-based simulation tool for cement hydration developed by Bentz and Garboczi [60,65–67]. In contrast to the vector models (i.e. off-lattice) described above, it uses a lattice-based approach based on digital images. A 3D cement paste microstructure is digitized onto a uniform cubic lattice and each volume element (or voxel) of the lattice is assigned to be some material (water-filled porosity, alite, etc.). Changes to the microstructure are simulated through a large number of rules that are evaluated locally and depend on the materials involved in the interaction, the temperature and, in some cases, global parameters describing the microstructure such as the water/cement mass ratio or the volume fraction of a phase. These rules are used to mimic the dissolution of solids, diffusion of dissolved species according to a random walk algorithm, and nucleation and growth of hydration products such as portlandite and C–S–H gel.

This lattice-based approach is well suited to simulate the spatial distribution of different phases, representing different shapes, and performing efficient calculations. Also, as the model is already in the form of discrete elements, this approach can be easily integrated with finite element methods for calculation of mechanical properties. Another advantage of this approach is that due to the regular nature of the mesh, most operations on the system are fast. Simulation of randomly shaped cement particles, reconstructed from X-ray tomography results, has also been included in the recent versions of the model [68,69].

Hydration within the CEMHYD3D model proceeds in repeated discrete cycles of dissolution, diffusion, and reaction. This approach leads to 3D microstructure development for ordinary portland cement pastes that has a realistic appearance (see Fig. 6) and a quantitatively reasonable spatial distribution of the unhydrated cement, combined hydration products, and capillary porosity [70].

A wide range of properties can be followed as hydration proceeds, including heat of hydration, phase volume fractions, chemical shrinkage, percolation of capillary porosity, and setting time. Moreover, the microstructure at any time can be input to finite element or finite difference models to calculate the effective DC conductivity [71], AC impedance spectra [72], liquid permeability [73], or elastic moduli [74]. The model has been applied with considerable

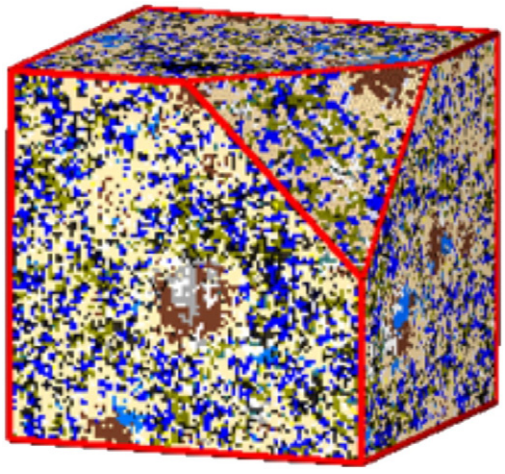

Fig. 6. CEMHYD3D simulated microstructure of a Type I ordinary portland cement paste hydrated for 14 days.

success to elucidate the influence of microstructural and environmental factors on hydration kinetics and microstructure development [75–77].

In spite of its many successes, the empirical reaction rules at the heart of CEMHYD3D present a number of inherent limitations. For example, the computational cycles possess no definite physical time scale. In particular, the time scale for the microstructure development must be calibrated to experimental data for each new cement mix, using some measure of the progress of hydration such as non-evaporable water content, chemical shrinkage, or calorimetry. Typically, this is done by assuming that the elapsed time t depends on the number n of computational cycles executed according to $t=\beta n^2$, with the scaling factor β being found by the best overall fit to the available experimental data. In addition, the rules are formulated to reflect basic information about the stability of ettringite, monosulfate, and hydrogarnet phases, but there is very little actual thermodynamic information in CEMHYD3D that can be used to predict the stable hydration products or how the stability is affected by the temperature or composition of the pore solution. Finally, it should be noted that the rules comprising CEMHYD3D were calibrated for a pixel size (i.e. lattice resolution) of 1 μm. Consequently, the simulations do not converge to any particular limit when the pixel size is systematically reduced; in other words, the model is not numerically convergent. The validity of using this relatively coarse lattice resolution for calculation of all these cement properties can be questioned, given the many important sub-micron aspects of cement and its hydration products. In fact, this limitation of CEMHYD3D was anticipated by its creators [78].

2.3.4. The HydratiCA simulation model

In response to CEMHYD3D's kinetic limitations, restricted applicability to different materials systems, and its lack of numerical convergence, a stochastic simulation model called HydratiCA has been developed by Bullard at NIST [79,80] that is based on more fundamental principles of kinetics of the individual rate processes comprising cement hydration. The HydratiCA model directly simulates (1) dissolution and growth of mineral phases, (2) diffusion of mobile species in solution, (3) complexation reactions among species in solution or at solid surfaces, and (4) nucleation of new phases. The principles of detailed balances and mass action are used to unify these disparate kinetic processes within a single simulation framework.

Each stoichiometric solid phase, such as C_3S or calcium hydroxide, is modeled as a separate chemical component, as are water and each aqueous solute species, such as Ca^{2+} or OH^-. These components are finely discretized into quanta of concentration called cells that are mapped onto a regular cubic lattice. The occupation number of cells of a given component at a particular lattice point determines its concentration there. For condensed phases, the concentration at a lattice site is directly related to its local volume fraction through its molar volume. The result is that the microstructure can be finely resolved both spatially and chemically. For example, in typical simulations the concentration of any solution component can be resolved within a 1-μm^3 volume to within 1 μmol/L.

Probabilistic rules are used to simulate chemical and structural changes over small time increments, each time increment being decomposed into independent transport and reaction steps. Diffusion is modeled as a random walk of cells between adjacent lattice sites, which can incorporate effects of solution nonideality and electrostatic interactions [79]. For chemical reactions among cells, the following rule for the probability of occurrence of a unit reaction in a time step Δt has been shown to yield kinetics that converge to the corresponding standard rate equation in the continuum limit [80,81]:

$$p_i = k\zeta^{\left(\sum_\alpha \nu_{\alpha,i}\right)-1}\Delta t \prod_\alpha \max\left(0, \prod_{m=1}^{\nu_{\alpha,i}} N_\alpha - m + 1\right) \quad (12)$$

where p_i is the probability of occurrence of a unit reaction of reaction i, k_i is the reaction rate constant for the reaction, ζ is the proportionality constant between occupation number N_α of species α and its molar concentration, and $\nu_{\alpha,i}$ is the molar stoichiometric coefficient of reactant α in reaction i.

A significant number of fundamental material parameters, such as molar volume and diffusive mobility, and reaction constants, such as the rate constant, equilibrium constant, activation enthalpy, and enthalpy of reaction, are required for input. However, there is no explicit dependence on mix design or cement clinker composition. In other words, one of the powerful motivations for developing this kind of model is that one does not need to adjust any of the reaction parameters to simulate different mixes. Instead, the differences between mixes, such as water–solids ratio, clinker composition, and particle size distribution, are specified at the beginning of the simulation through the assignment of the cell types and numbers at each lattice site.

HydratiCA makes more detailed predictions of the kinetics of phase changes and microstructure development as a function of solution chemistry and temperature than other microstructure-based models of hydration. However, this level of kinetic detail and accuracy makes the approach quite computationally intensive. Simulations of early-age hydration typically require very small time steps, about 0.2 ms, to ensure numerical stability because the electrolyte diffusion and precipitation reactions occur at rapid rates. Therefore, about 18 million steps are required to simulate just 1 h of hydration. For slower processes like sulfate attack of mature binders, much longer times could be simulated with the same computational resources.

HydratiCA has been used to investigate the plausibility of various possible mechanisms of hydration of tricalcium silicate [52,82] and tricalcium aluminate, both of which are important minerals in all ordinary portland cement pastes. Recent application of HydratiCA to simulate early-age hydration kinetics is discussed in Section 3.2.

2.3.5. The μic microstructural modeling platform

The recently developed μic (pronounced “mike”) microstructural modeling platform [59] is derived from an earlier model developed by Navi and Pignat [83], which was in turn based on the original vector model of Jennings and Johnson discussed above. While μic still uses the growth of multilayered spherical particles and their assemblages to represent the microstructural evolution, it provides a new implementation to the vector approach that addresses some of the limitations of its predecessors. Because the calculation of overlaps or distances between particles, even spherical ones, can be computationally intensive, earlier implementations of the vector approach chose either to limit the number of particles [83] or not to calculate those overlaps at all [62], severely affecting the performance of these models. The new support libraries developed for the platform allow μic to model the hydration of millions of cement particles, needed to realistically represent the particle size distributions found in contemporary cements, taking the condition and neighborhood of each particle into account. Typical simulations on μic with a few million particles take a few hours on single-processor desktop computers.

Recognizing that there are several important aspects of cement hydration that are still not well understood, μic allows the user to fully customize the simulations. To run a simulation on μic, the user first defines all the phases and the stoichiometry of the reactions to be simulated. The user can define whether the phases are interspersed with another phase, as separate particles or as a concentric layer around other phases and the relative position of these layers. The initial particle size distribution and the phase composition of the powders are also defined by the user.

The simulations can then be customized using plugins, which are encapsulations of algorithms or models that can be loaded by μic at run-time and used as an integral part of the model. The user can choose from a library of plugins of the most commonly used models,

or create their external plugins for their own models. The plugins have access to all the microstructural information and support libraries available in μic and can be used to control various aspects of the simulations such as the initial particle packing, reaction kinetics and triggers (i.e. special rules required to simulate the activation of particular mechanisms or chemical reactions), the distribution of a product to different particles, the variation of the density of a phase and the rate and location of creation of new particles.

In general, μic is well suited to investigating various phenomena at the microstructural level, such as the distribution of hydration products and the effect of particle size, since the simulations can be compared directly with experimental data such as isothermal calorimetry curves [84]. It is important to note that μic does not directly account for solution phase chemistry, which provides the thermodynamic driving force for microstructure changes, or transport phenomena such as diffusion, which provide interactions between phases, thus influencing the distribution of hydration products. However, plugins can be devised either to model the overall effect of these phenomena on individual particles or to enable external programs such as HydratiCA [79] or GEMS [85,86] to provide μic with the necessary information. Still, it must be ensured that the results obtained are indeed a consequence of the processes simulated and not a side effect of the assumptions made while formulating the models.

The speed and flexibility of μic allow for the simulation of systems with a large range of particle sizes, such as cements with fine fillers (Fig. 7, left) and cases where very specific mechanisms are to be modeled, such as the nucleation of a phase on the particles of another phase (Fig. 7, right). Although new users may find the platform difficult to use due to the large number of customizable elements, this flexibility allows μic to be used as a tool to study mechanisms and to verify the validity of hypotheses and models. An application of μic to analyze the early hydration kinetics of alite is discussed in Section 3.3.

3. Recent advances in kinetic modeling

3.1. Analyzing C_3S hydration kinetics and the effects of $CaCl_2$ using the boundary nucleation and growth model

As was discussed in Section 2.2, the mathematical boundary nucleation and growth (BNG) model is a modified version of the JMAK model that assumes that nucleation is restricted to internal boundaries within the transforming system. This provides a better physical analogy to C_3S or cement hydration, such that values for specific physical parameters (rather than just averaged rate constants) can be obtained. This adds greatly to the utility of the nucleation and growth modeling approach, and allows the applicability of the model to be tested. Because of the codependence of G, I_B, and O_v^B, all three cannot be determined from the fitted values of the rate constants k_B and k_G. However, the value of O_v^B can be estimated from an independent measurement of the powder surface area, allowing G and I_B to be determined. For pure C_3S hydrated at 20 °C, Thomas [46] found that $G = 0.08$ μm/h and $I_B = 0.068\ \mu m^{-2} h^{-1}$. The linear growth rate has also been measured directly by observing the growth of hydration product on a flat C_3S surface using AFM [87], resulting in values of $G = 0.065$ μm/h parallel to, and $G = 0.148$ μm/h perpendicular to, the surface. While directional dependence of the growth rate is not incorporated in the BNG model, the agreement, particularly given the multiple sources of uncertainty involved in the comparison, is encouraging. The authors are not aware of any direct measurements of the nucleation rate on the C_3S particle surface, but such measurements can in principle be made.

As shown in Fig. 3, BNG fits to calorimetry data from $CaCl_2$-accelerated pastes provide a much better fit to the extended post-peak regime than for neat paste systems. In this case, the growth rates were similar to those measured for pure C_3S at the same temperature, whereas the nucleation rates were some 10–30 times higher. Thus based on these fits it appears that $CaCl_2$ accelerates hydration by increasing the rate of nucleation on the C_3S surface (I_B), so that more regions of hydration product are growing at the same time, but that the rate of growth of each individual region (G) is relatively unaffected.

The proportionality constant, A, used to convert the dimensionless volume fraction, $X(t)$, of the nucleation and growth models to the calorimetry units of kJ of heat evolved per mole of C_3S, was significantly higher in the presence of $CaCl_2$ (e.g., 42 kJ/mol vs. 92 kJ/mol for one batch of C_3S at 20 °C [50]). The parameter A represents the total amount of hydration occurring by the nucleation and growth process, and can be converted to the degree of hydration of the C_3S by dividing it by the specific heat of C_3S hydration (121 kJ/mol); this results in values of $\alpha = 0.35$ for C_3S and $\alpha = 0.76$ for $CaCl_2$-accelerated C_3S for the above example. Thus the model predicts that the nucleation and growth process encompasses only a fraction of the overall hydration of C_3S (in the case of pure C_3S, the low value of α also arises due to the deviation between the data and fit). Since the model is based on the filling of the available space with hydration product, the implication is that the space is filled well before the C_3S has fully reacted. However, for the w/c used for these experiments (0.5) the C_3S will hydrate completely at long times. Thomas et al. [50] suggested that not all of the capillary pore space was available for hydration product, and that the C–S–H gel formed

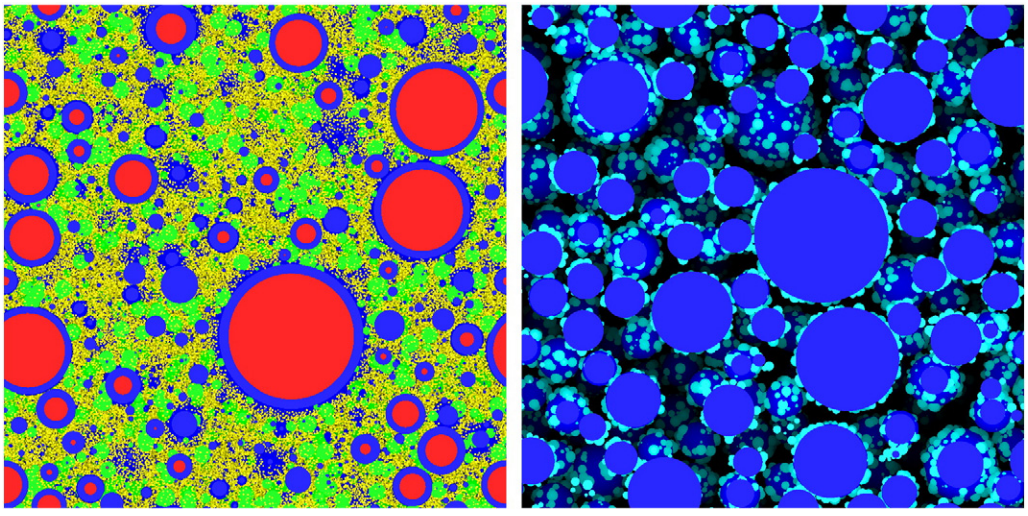

Fig. 7. Simulations of microstructures with fine fillers and large number of particles (left) and controlled nucleation on surface of particles (right), simulated using the modeling platform μic.

initially with a low bulk density such that the available space was filled at a low degree of hydration. According to this hypothesis, the C–S–H bulk density with pure C_3S hydration is particularly low at early times, but increases after the main hydration peak, causing the deviation between the BNG fit and the data. Bishnoi and Scrivener [84] independently proposed a similar mechanism to explain the early hydration kinetics of pure C_3S (see next section). However, other explanations are possible, as discussed in Section 5.

The BNG model was also recently used to fit the chemical shrinkage of Class H oil well cement, which has high C_3S and low C_3A content [88]. As shown in Fig. 8, the fit is good for the derivative (rate) curve, even though the fit was applied only to the cumulative shrinkage. Similar fits were obtained for hydration at temperatures from 10 °C to 40 °C, w/c from 0.25 to 0.4, and for pastes with a variety of accelerators and retarders.

When the degree of reaction is small, Eq. (7) reduces to

$$X(t) \approx k_B^4 t^4 \approx O_v^B I_B G^3 t^4. \quad (13)$$

Based on measurements of α by thermogravimetric analysis and initial setting time, t_{set}, by Vicat needle, it was found that $X(t_{set})$ is constant [88], so Eq. (13) indicates that t_{set} should be inversely proportional to k_B. As shown in Fig. 9, this is valid for Class H cement at w/c = 0.35 over a range of temperatures, with and without accelerators and retarders. Eq. (13) has been successfully applied to predict the change in setting time with pressure, as well as temperature [51].

The BNG model can be modified to allow for growth from a fixed number of nuclei (site saturation) rather than continuous nucleation [53], which better matches the results of HydratiCA simulations conducted by Bullard [52]. In this case, the fits to the chemical shrinkage data from ref. [88] are slightly better, except for the data obtained at 60 °C. The fact that two different versions of the model give similar fits means that one cannot use the quality of the fit to prove the validity of the model, unless independent data are available. Further work comparing the different BNG fits to chemical shrinkage and calorimetry data from the same pastes is planned, including testing the confined growth models of Villa and Rios [55].

3.2. Insights on early-age kinetic mechanisms using HydratiCA

HydratiCA is distinguished from other hydration simulation models by its ability to incorporate the influence of solution chemistry, temperature, and thermodynamic variables on the kinetics of early-age hydration and microstructure development. This ability is a major advance in modeling capability because the solution

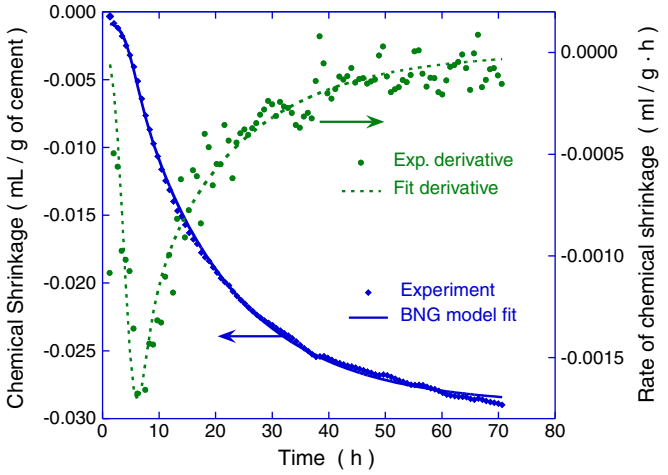

Fig. 8. Fit of BNG model to chemical shrinkage data for Class H cement, w/c = 0.35, T = 25 °C [88]. Only the cumulative shrinkage was used in the fit, but the derivative is accurately captured until well beyond the peak.

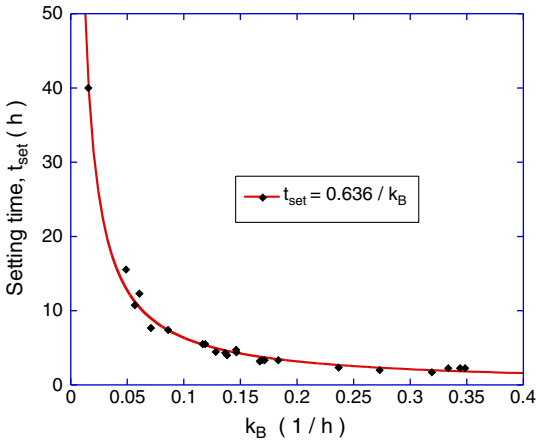

Fig. 9. Inverse relationship between initial setting time (found by Vicat needle test) and k_B found by fitting BNG model to chemical shrinkage. Data are for Class H cement, w/c = 0.35, hydrated at temperatures from 10 to 40 °C, with and without accelerators and retarders [88].

composition determines the thermodynamic driving force for dissolution of clinker phases as well as the nucleation, growth, and stability of hydration products, and also for the composition of non-stoichiometric phases such as C–S–H gel.

It should be emphasized that many of the properties that determine early-age cement hydration kinetics and microstructure development, such as the nucleation energy barriers and rate constants for dissolution of clinker phases and growth of hydration products, have not been measured to our knowledge. Nevertheless, in the absence of measured values, HydratiCA has been used to investigate the plausibility of various proposed, but unproven, mechanisms of hydration by using reasonable estimates of these material properties. For example, HydratiCA was recently used to make a quantitative demonstration that a thin, passivating layer of C–S–H on C_3S surfaces could explain not only the unusually slow dissolution rate of C_3S during the so-called induction period, but also the evolution in pore solution composition, the nucleation of a more stable form of C–S–H, and its effect on destabilizing the semipermeable layer and accelerating C_3S dissolution [52]. To simulate the observed compositional variability of C–S–H, two different stoichiometric compositions of C–S–H were assumed, one with Ca/Si = 1 and the other with Ca/Si = 2 on a molar basis. These two different forms behave like end members of a solid solution range of Ca/Si values. However, the only way to fit the experimentally observed hydration rates using the passivation layer mechanism was to assume a different effective diffusivity for each end member. Although very different morphologies of C–S–H can be observed in cement paste microstructures, there is no evidence that these morphologies are linked to composition in the way assumed in these simulations.

More recently, HydratiCA simulations were performed using a newer "slow dissolution step" hypothesis, which assumes that no layer forms on the C_3S surface, but that active dissolution sites at surface defects are deactivated as the driving force for dissolution is reduced [89–91]. These simulations also agree well with experimental data without having to assume markedly different diffusivities for the end members of the C–S–H composition range [82]. As an additional test, both dissolution mechanisms were compared in simulations where portlandite was prevented from forming at any time. When the slow dissolution step mechanism was used, the slow reaction period was extended by several hours when portlandite formation was suppressed, as shown in Fig. 10. The slow dissolution step hypothesis therefore can help reconcile the interpretation of seemingly contradictory sets of experimental data in the literature [92,93]. In contrast, the simulations showed that the passivation layer hypothesis predicts that calcium hydroxide nucleation and growth should have no significant effect on the length of the induction period. The different

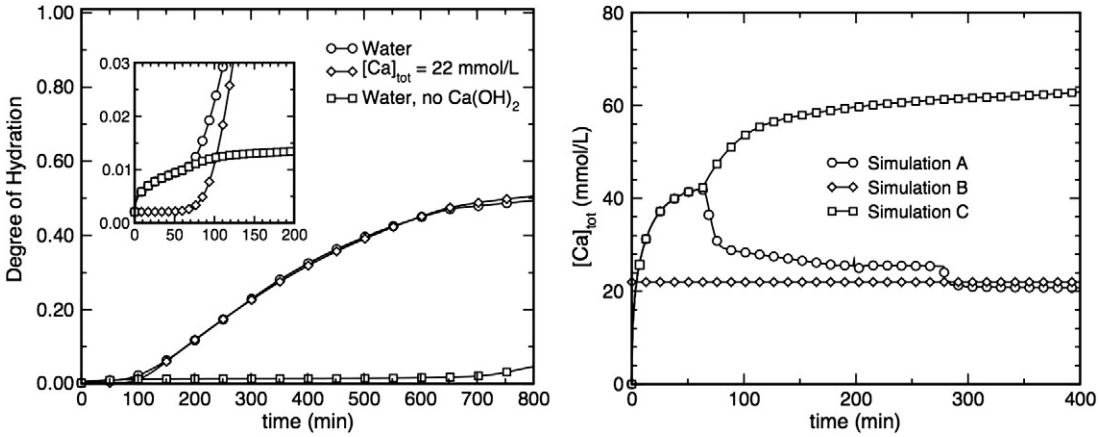

Fig. 10. HydratiCA simulations of C_3S hydration showing the predicted effect on hydration rate (left) and solution composition (right) of suppressing the precipitation of CH (open squares) in contrast with buffering the solution with calcium at 22 mmol/L (diamonds) or allowing CH precipitation to occur naturally (from [82]).

predictions of the two hypotheses could potentially be used to distinguish between them experimentally by artificially elevating the calcium concentration in solution and noting the effect on the induction period [82].

Many of these kinds of mechanistic investigations can be made on relatively small computational systems, such as a single cement particle immersed in a sufficient volume of water to give a desired water-to-cement mass ratio (w/c). However, recently HydratiCA has been modified to run on multiple parallel processors, which enables it to access much larger system volumes via spatial decomposition of the computational domain [94]. Simulations have been made of ternary $C_3S + C_3A +$ gypsum systems in water with several dozen particles having realistic size and shape distributions. The simulations have investigated the development of spatial correlations of hydration products like ettringite and calcium hydroxide with dissolving cement phases like C_3S, C_3A, and gypsum.

Because the growing and dissolving phases are somewhat linked by the diffusive transport of ions through solutions, it is reasonable to expect that hydration products will tend to be located near those dissolving phases that provide ions they need for their growth. HydratiCA simulations suggest that ettringite is correlated with C_3A but not gypsum, presumably because of the common calcium and aluminate components of each, and that calcium hydroxide is also correlated more strongly with C_3A than with C_3S, as shown in Fig. 11. This latter phenomenon seems to be due to volume exclusion of C–S–H gel around C_3S grains rather than any particular chemical tendency of the calcium hydroxide to prefer C_3A [94].

3.3. Analyzing early hydration with μic

The modeling platform μic [59] has recently been used to study the early age hydration of alite [84]. Although analytical and numerical models have been previously used to study alite [47,95], the unique capability of μic to incorporate user-defined models for reaction of each particle in large systems and to explicitly consider overlaps between all particles has allowed a deeper investigation of existing theories. In this study, isothermal calorimetry measurements of the hydration rate of alite powders with different particle size distributions [96] were compared with μic simulations incorporating different models of possible reaction mechanisms.

Simulations of the growth of spherical nuclei on the surface of spherical substrate particles indicate that impingement between nuclei growing on the same substrate particle is not sufficient to reproduce the rates of deceleration observed for cement; substantial impingement between growing nuclei originating on different substrate particles is required. Simulations using particle size distributions close to those studied in the laboratory were performed. These showed that if the bulk density of C–S–H is assumed to be close to 2.0 g/cm^3 [97], as is usually reported in literature, then although the acceleration can be modeled by considering the growth of C–S–H nuclei on alite particles, the subsequent deceleration cannot be reproduced. This is because the volume of C–S–H produced by the time of the rate peak is not sufficient to cause impingements with C–S–H growing on neighboring alite particles.

The so-called "diffusion hypothesis" [47], which holds that the deceleration period begins when resistance to the flow of ions provided by the layer of C–S–H growing on the alite particles becomes the rate-controlling step, was also investigated through μic simulations. In this case, it was found that the experimentally observed decelerations can be simulated only if the transport properties of C–S–H are assumed to vary strongly with the size of the particle on which it forms. As there is no physical basis for this dependence on particle size, the simulations do not support this hypothesis.

Based on the observation that the volume of C–S–H was insufficient to cause impingement with C–S–H growing on neighboring alite particles and hence a deceleration, it was proposed that during the early hours of hydration C–S–H grows in a loosely packed manner and then densifies at later times. This hypothesis was investigated with μic and it was found that good fits were possible, supporting the possibility of such a mechanism being active in alite hydration. However, the required initial bulk density of C–S–H was found to be quite low, in the range of 0.2 g/cm^3, which is equivalent to less than 10% packing density of C–S–H gel particles, based on the solid density values given by Allen et al. [98]. An important observation is that in order for the simulated rate peak to occur at the correct time, the early rate of growth of the C–S–H nuclei must be relatively high and be proportional to the available space between the hydrating particles. If this is the case, then loosely-packed C–S–H would tend to fill a large part of the microstructure in the early hours of hydration. Micrographs showing the presence of such a loosely packed C–S–H filling a large part of the microstructure by the peak of hydration and other independent evidence such as SANS measurements [50] appear to support the hypothesis. While this study points out practical difficulties associated with the various scenarios that have long been proposed for alite hydration, more investigation into the hypothesis of a loosely packed C–S–H phase at very early times is needed.

These kinds of investigations demonstrate that μic has the desirable ability to quickly assess different "what-if" scenarios, where implications of certain assumptions about overall reaction rates or material properties can be checked and used to stimulate further experimental research. Therefore, μic can represent an important part of a multiscale simulation approach in which its kinetic rules can be better informed by simulations at finer length and time scales using HydratiCA or atomistic methods.

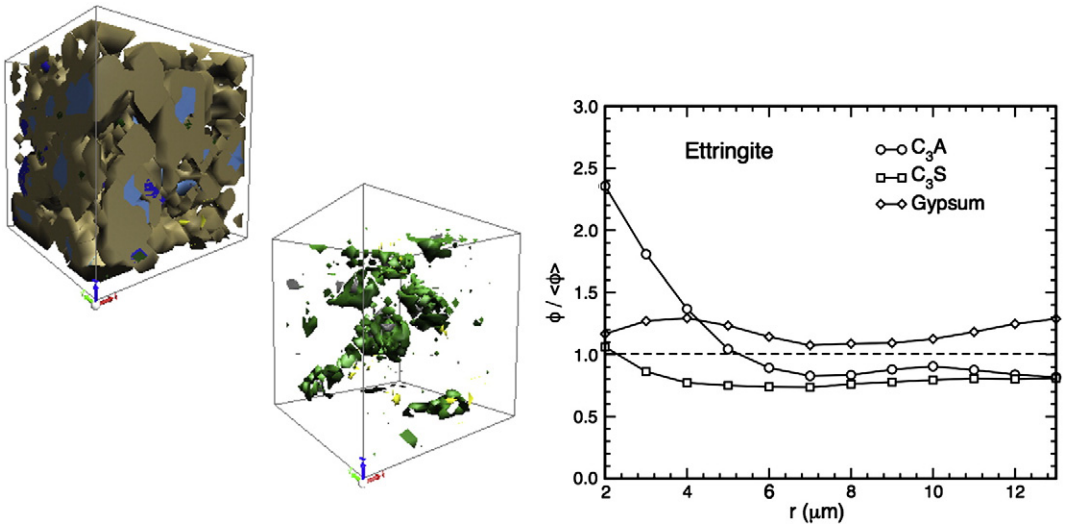

Fig. 11. HydratiCA simulations of an idealized portland cement paste. Upper left image is the microstructure after 180 min hydration (light blue is C_3S, dark blue is calcium hydroxide, brown is C–S–H, gray is C_3A, green is ettringite, and yellow is gypsum). Lower right image is the same microstructure with the silicate phases removed to reveal the minority aluminate phases. The plot on the right shows the calculated radial distribution functions for ettringite as a function of distance from surfaces of C_3A, C_3S, or gypsum, and reveals quantitatively the tendency for ettringite to precipitate near C_3A surfaces but not near gypsum or C_3S surfaces (from [94]).

4. Molecular modeling of specific hydration steps

The models and simulation methods described in the previous sections are capable of generating considerable insight into hydration kinetics, microstructure development, and the implications of these for the changing physical properties of cement paste and concrete. However, such models require, to varying degrees, input of data on thermochemical, physical, and structural properties of the constituent materials, as well as reaction rate data. Such data must be obtained outside these models, either from experiments or from more fundamental calculations of these quantities using molecular-scale techniques. This section discusses the recent applications of a number of molecular-scale simulation methods to cementitious materials.

Molecular-scale simulations (also called atomistic simulations), whereby materials are simulated at the atomic level by modeling the forces that bind the atoms together, are of great importance for the understanding of materials. In theory, any chemical reaction or physico-chemical property of a material (including C–S–H gel and other cement phases) can be explained and modeled in terms of changes in the atomic and electronic configuration of the system. It is clear, therefore, that these methods can provide important information regarding activation energies, possible reaction pathways, conformational analysis, spectroscopic and mechanical properties, and diffusion and transport-related properties. All of these are related in some way to microstructure development and kinetics.

The use of atomistic simulations for cementitious materials is a new field, and probably less known than the methods described in previous sections. For this reason, before discussing the recent application of a number of molecular-scale simulation methods to cementitious materials, a brief background summary is provided in Section 4.1. Section 4.2 then describes progress in performing atomistic simulations of the C–S–H gel phase, while Section 4.3 illustrates the potential ability of atomistic simulations to provide a novel computational scheme for describing the dissolution of C_3S and related phases.

It is worth noting that molecular modeling studies done to date have focused primarily on the structural properties of the cementitious phases, rather than the intrinsic kinetic aspects of cement hydration. However, the accurate structural information gained from these atomistic modeling studies may serve as valuable input for the kinetic models. It is also clear that molecular modeling techniques are, in principle, well suited to describe the processes that control the kinetics. This fact is indeed exploited in other fields, such as geochemistry, where atomistic simulations have successfully simulated the dissolution and growth processes occurring in minerals.

4.1. Atomistic simulation methods

Atomistic simulations of fundamental chemical reaction steps are typically classified into two different categories: quantum mechanical (QM) simulations and force field (FF) Methods. QM simulations (also called first principle or *ab-initio*) explicitly represent the electrons in the calculation. This renders them computationally expensive, but allows them to simulate properties that depend upon the electronic distributions. Therefore they can model chemical reactions in which bonds are broken and formed.

Two main QM approaches exist, known as Hartree–Fock (HF) and Density Functional Theory (DFT). HF methods directly tackle the Schrödinger equation to solve the wave function of the electrons and nuclei of the system of interest. These calculations average the electron–electron repulsion and provide an exact means of treating the electron exchange, but they fail to adequately represent electron correlation (the fact that electrons in a molecular system react to one another's motion and keep out of one another's way). Post-HF methods correct this shortcoming by adding new contributions to the electron correlation, though at a computational expense.

Density Functional Theory (DFT) simulations rely on the existence of a relationship between the total electronic energy and the overall electronic density. Hohenberg and Kohn [99] demonstrated that the ground-state energy and other properties are unequivocally defined by the electron density. Afterwards, Kohn and Sham [100] suggested a practical way of solving the Hohenberg–Kohn theorem, leading to a self-consistent set of equations named “Kohn–Sham equations”. Within this theoretical framework, the intractable many-body problem of interacting electrons is reduced to a tractable problem of non-interacting electrons moving in an effective potential. As this effective potential includes the effect of electron exchange and correlation interactions without the additional computational cost of post-HF schemes, DFT methods are especially attractive [101].

In contrast to the QM schemes described above, FF methods ignore the electronic motion and calculate the energy of the system as a function of the nuclear positions. The atoms are treated as classical entities that interact through semi-empirical interaction potentials that are developed based on physical insights. These potentials are designed to mimic, for example, Coulombic interactions, dispersive attractions, short-range repulsive forces, and even covalent bonds. FF simulations cannot provide information that depends upon the electronic structure, but they can be as accurate as the QM simulations for other properties provided the empirical potentials are good enough. Their principle advantage is that they are computationally less expensive, and can therefore cope with larger systems containing ~10^5–10^6 atoms, in contrast to the QM simulations that are currently limited to ~10^2 atoms.

Central to both QM and FF simulations is the concept of the energy surface. Assuming that the movement of electrons is sufficiently fast that they can rearrange into their ground state configuration for a given position of the nucleus (the Born–Oppenheimer approximation), the energy of the system can be expressed as a function of the atomic positions. The minimum (lowest energy) configuration is known as the *global energy minimum*. Different minimization or "relaxation" techniques have been devised (see e.g. [102]) to identify those geometries that correspond to the lowest points on the energy surface. These represent the most stable states of the system at absolute zero temperature. When finite temperature effects are also considered, the goal is not to find the global energy minimum but to appropriately sample the energy surface so as to reach the equilibrium configuration. For instance, in the case of classical particles the equilibrium configuration corresponds to a Boltzmann distribution, where the probability of a state with energy ε_i and temperature T is proportional to $e^{-\varepsilon_i/k_BT}$, where k_B is the Boltzmann constant.

Two main procedures are used to sample the energy surface and search for the equilibrium configuration. Monte Carlo (MC) simulations generate configurations of a system by making "smart" random movements of the atoms, while Molecular Dynamic (MD) simulations follow the physical time evolution of system by integrating Newton's laws of motion. Classical MD simulations employ FF interatomic potentials to describe the interaction between the particles, whereas quantum or *ab-initio* MD simulations (QMD) are based on a quantum description of the interactions. In this last case, the forces are calculated by evaluating the electronic total energy and interatomic forces at each time step, such as by using Car–Parrinello algorithm [103] or through direct minimization of the electronic total energy on the potential energy surface (the so-called adiabatic or Born–Oppenheimer molecular dynamics). The total configurational energies at each MC step can also be calculated by either FF or *ab-initio* methods. In any case, MC methods tend to find the equilibrium configurations more quickly than MD simulations, but in their usual implementation they are not deterministic and cannot simulate time-related properties. MD simulations can effectively address dynamical properties, though at present this is typically limited to a few nanoseconds in elapsed time.

This limitation in the accessible simulation time represents a substantial obstacle whenever the processes of interest take place over a time scale that is several orders of magnitude slower than atomic vibrations, which is often the case. Several sophisticated models like the mature Kinetic Monte Carlo (KMC) scheme (e.g. [104]) and the relatively recent Accelerated Molecular Dynamic (AMD) method [105] have been developed to overcome this time scale problem. Both methods are based on stimulating state-to-state diffusive jumps while keeping an appropriate time assignment for each state-to state transition. These two promising tools are capable of simulating processes on the scale of microseconds, or even seconds in some favorable cases, and currently offer a good computational framework for studying kinetics. A simple schematic showing the typical length and time scales accessed by each of the atomistic methods discussed above is given in Fig. 12.

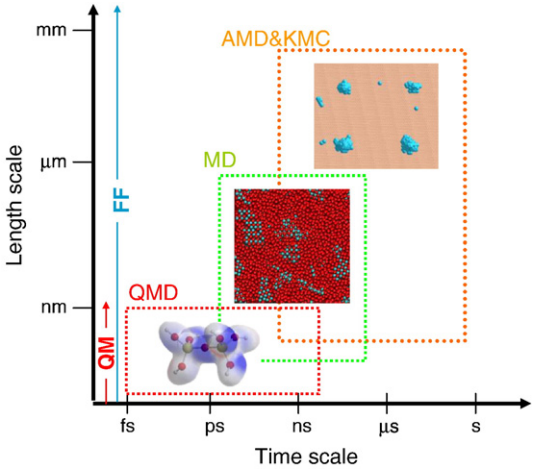

Fig. 12. Schematic illustrating the typical length and time scales accessible by various types of atomistic simulations discussed in the text.

4.2. Atomistic simulations of C–S–H gel

C–S–H is a poorly crystalline phase with variable stoichiometry in terms of both its calcium content (Ca/Si ratio) and water content (H_2O/SiO_2 ratio). Furthermore, the molecular ordering of C–S–H is still under debate, so atomistic simulations of C–S–H cannot benefit from a well-defined starting structure, as is the case for nanocrystalline alloys and metals. As such, C–S–H gel presents a significant challenge for atomistic modelers. Nevertheless, the effort and interest aimed at obtaining an accurate atomistic description of C–S–H gel are recently increasing. This may be attributed to a growing belief among cement chemists that obtaining a deeper understanding at the atomic level is necessary before achieving the goal of controlling and designing the properties of concrete [106].

While at the nanostructural level C–S–H gel does not show long-range crystalline order and has many properties associated with colloids [107,108], it is generally believed that at the atomic level it contains many structural features in common with the layered minerals tobermorite and jennite. As atomistic simulations are especially well suited for application to crystalline structures, much work has been carried out on these minerals, under the assumption (or hope) that the results would provide insight into the chemistry of C–S–H gel. For example, Churakov [109] recently studied the hydrogen bonding scheme of jennite by *ab-initio* molecular mechanics, obtaining results in agreement with the proton assignation made by Bonaccorsi et al. [110] based on XRD measurements. These simulations found that the outermost external oxygen atoms of the bridging silicate tetrahedra remain basically de-protonated, and thus act as acceptors for both hydrogen bonds and cations.

Churakov also recently analyzed the hydrogen network of normal and anomalous 11 Å tobermorite [111,112], a tobermorite polytype that has also been studied by others [113,114]. Starting from previously proposed structures [115,116], Gmira et al. [113] and Pellenq et al. [114] performed force field simulations and *ab-initio* simulations to obtain information about the cohesion of the 11 Å tobermorite layers. The simulations demonstrated that, contrary to what happens in smectite clays, the calcium ions and water molecules present in the interlayer spaces are not exchangeable since they are trapped by strong iono-covalent forces; i.e. the interlayer Ca ions are chemically similar to those bound into the main layer. This finding may have direct bearing on the cohesion of C–S–H gel, since if C–S–H gel is made up of tobermorite-like bricks, the contacts between the bricks should be governed by strong cohesive forces similar to those binding the tobermorite layers together.

A simple manifestation of the cohesive forces that bind a phase together is the phase's response to external loads. Atomistic simulations can easily determine the elastic tensor coefficients of crystalline structures, since the stress components can be written as a second derivative of the energy with respect to strain, and this allows elastic moduli to be calculated from first principles. Manzano [117] discussed in detail how this approach has been used to determine the elastic properties of 21 crystalline minerals related to C–S–H. For C–S–H gel itself, nanoindentation studies [118] have determined that the elastic modulus of the solid C–S–H particles is about 60 GPa. The modulus values found in the literature for 14 Å tobermorite and jennite [114,119,120] agree with this value, which supports the hypothesis that they are good C–S–H analogs. The moduli for 11 Å and 9 Å tobermorites are higher, in the range of 75–95 GPa [114,119,120], presumably due to their smaller interlayer spacing, which leads to greater cohesion.

In contrast to the above work, some atomistic simulations aimed at modeling C–S–H formation have exploited various features present in the layered structure of tobermorite and jennite crystals without incorporating their entire crystalline structure. Manzano et al. [121] identified a possible precursor of tobermorite, jennite, and C–S–H consisting of two silicate chains sandwiched by a single calcium oxide layer. Increasingly complicated structures were obtained by aggregating these units with calcium ions. Interestingly, two different growth mechanisms were identified that, depending on the amount of Si and Ca ions, naturally lead to either tobermorite-like or jennite-like dimeric units (T_2 and J_2). While the dipole moments found for the T_2 units are relatively low (3.4–1.7 Debyes), those of the J_2 units are much higher (above 25 Debyes). It was suggested that this high dipole value enables the formation of still larger and more ordered structures through dipole–dipole interactions.

Another group of researchers [122,123], assuming that C–S–H gel has a layered structure, used atomistic Monte Carlo simulations to gain insight into the electrostatic attraction between layers. They simulated the structure of C–S–H as structureless charged lamellae embedded in a counterion-rich electrolyte solution. Interestingly, their results revealed for the first time the need to include the atomistic description to explain the attraction of charged plates (lamellae) neutralized by exchangeable counterions. In contrast to previous attempts based on the classical Derjaguin–Landau–Verwey–Overbeek (DLVO) method, their simulations captured the ionic correlations present in divalent solutions and provided a partial explanation for the cohesion of C–S–H particles. Other studies [124] have likewise corroborated the same idea by similar methods. However, in view of the results of later work [114] it appears that while such ion correlation forces are significant on a colloidal scale, the most important contribution to the cohesion actually comes from strong iono-covalent forces that act at the scale of the contact zones between C–S–H bricks.

Ayuela et al. [125] and Manzano et al. [126] used DFT calculations to study the stability of the (alumino)silicate chains in C–S–H gel. The only structural constraint imposed on the simulations was the *dreierketten* arrangement of the chains. By analyzing the energies involved in the condensation reactions, they obtained results in agreement with experimental evidence showing that the most stable (alumino)silicate chains in C–S–H gel have chain lengths $m = 3n - 1$, where n is a positive integer.

The first attempt to accomplish the difficult task of describing the formation of C–S–H gel without imposing any structural constraints was that of Dolado et al. [127]. They used MD simulations to follow the polymerization of silicic acid, $Si(OH)_4$, in the presence of hydrated portlandite molecules ($Ca(OH)_2$ $4H_2O$). By counting the number of Si–O–Si, Ca–OH, and Si–OH bonds that formed, the similarity to 1.4-nm tobermorite and jennite could be assessed. Their results indicate that at low Ca/Si ratios the simulated C–S–H systems can be seen as mixtures of long polymerized (pentamers and longer chains) 11 Å tobermorite, 14 Å tobermorite, and jennite structures, whereas at high Ca/Si ratios they seem to be composed of short (dimeric) 14 Å tobermorite and jennite pieces. The same computational scheme was later employed [128] to analyze the incorporation of Al atoms into C–S–H gel. In this study different amounts of $Al(OH)_3$ and $Na(OH)\cdot 5H_2O$ molecules were added to the "soup" of $Si(OH)_4$ and $Ca(OH)_2$ $4H_2O$ molecules to follow by MD simulations the formation of C–A–S–H particles. These simulations succeeded in reproducing experimental evidence that the Al atoms lengthen the chains and promote the appearance of three-dimensional structures.

Pellenq et al. [129] recently developed a molecular model for C–S–H gel from which various observations such as NMR, IR, and X-ray spectra can be calculated. Initially, they modified the structure of dry 11 Å tobermorite to account for the higher Ca/Si and shorter silicate chains observed in C–S–H gel. They then performed Grand Canonical Monte Carlo simulations of water adsorption, coupling the defective structure to an external reservoir at a chemical potential corresponding to liquid water at 300 K. Their structural analysis recognized that water molecules can be adsorbed, not only in the interlayer space, but also in small holes present in the defective structure. At equilibrium, the composition of their structure ($C_{1.65}$–S–$H_{1.75}$) is close to the experimental value for solid C–S–H ($C_{1.7}$–S–$H_{1.8}$) provided by neutron scattering measurements [98]. However, the model density (2.56 g/m^3 before, and 2.45 g/m^3 after, final relaxation of the structure [129]) is lower than the corresponding neutron scattering value of 2.60 g/m^3 [98]. Thomas et al. [130] have recently pointed out that the atomic packing density of C–S–H is higher than that of its mineral analogs tobermorite and jennite, causing its mass density to be higher than expected. The structural reason for this high atomic packing is an ideal question for molecular modeling efforts to address.

4.3. Dissolution of C_3S and related minerals—ab initio calculations and parameterized Monte Carlo techniques

As the initial step in the hydration process, dissolution of the cement minerals plays an important role in controlling the hydration kinetics, particularly the initial slow reaction period often called the induction period (see review of hydration mechanisms in this issue [1]). However, relatively little attention to date has been paid to the mechanisms and rate by which the more soluble cement minerals such as C_3S dissolve into the pore solution. Processes that change the surface topography of minerals such as adsorption, desorption, dissolution, and growth reactions are difficult to observe directly at atomic scales. This problem is particularly acute for sophisticated analytical methods, such as atomic and scanning force microscopy (AFM and SFM) and vertical scanning interferometry (VSI) (e.g. [131]). Even if the necessary spatial resolution can be achieved, the primary limitation is adequate time resolution.

For this reason, theoretical considerations and molecular modeling techniques such as kinetic Monte Carlo (KMC) methods are the tools of choice to extend investigations to the molecular scale. KMC methods can also provide direct feedback and help interpret observations of crystal surfaces made with VSI and other methods. The ability to compare, for example, the evolution of a virtual crystal surface with the experimental result at high, i.e., molecular resolution is a major strength, and allows reinforcement and testing of the KMC parameterization (e.g., [132]). A key factor in the success of this approach has been rapid increases in computing power. Cygan and Kubicki [133] have assembled a comprehensive overview of the modeling work. Significant further advances have been made during the last few years by Casey and coworkers [134,135].

The approach that is discussed here involves the complementary use of two techniques: *ab initio* and KMC simulation methods. This approach has had success in treating geochemical processes such as mineral dissolution and growth [136–143], and thus holds promise for treating the combined dissolution and growth processes active in cement hydration. Other modeling techniques, such as lattice dynamics (LD) and molecular dynamics (e.g., [144]) and Lattice

Boltzmann methods have also been applied successfully to geochemical problems. It should be stressed that these modeling techniques develop their full potential when they are used in combination with experimental and analytical strategies (see [145]).

The KMC technique allows us to explore the processes of crystal dissolution and growth at the atomic/molecular scale using a system size that is orders of magnitude larger than can be covered by *ab initio* models (e.g., [143]), which is the rationale for combining this method with *ab initio*/density functional calculations (DFT). For a comprehensive overview and in-depth discussion of KMC simulation and its application in geochemical studies see Lasaga et al. [146,147]. Gilmer [148–150] used this technique successfully to study crystal growth in the 1970s, and during the following decade Lasaga and co-workers applied Monte Carlo techniques to the study of crystal dissolution (e.g., [151–153]).

While earlier studies explored dissolution kinetics of mineral surfaces often in relatively crude molecular block models (e.g., [136,137]), the rapidly increasing speed of computers and new theoretical concepts today permit crystal dissolution and growth to be simulated using real crystal structures with complex lattices, solid-solutions, order–disorder phenomena, dislocations, and the pH value of the aqueous solution (e.g., [140–142]). An important milestone was the derivation of the so-called stepwave model [136,137] of crystal dissolution. This model provided the basis for further theoretical study of crystal dissolution and growth [138,140–142]. Recently, Meakin and Rosso [143] expanded the system size of such KMC simulations significantly by developing new and faster algorithms.

KMC techniques treat crystal dissolution or growth as a many-body problem and, therefore, as a stochastic process in which random events generated by a probability distribution function are observed and counted. In the case of crystal–fluid interactions, the rates of microscopic processes such as bond breaking/formation are translated into probabilities (e.g. [154]). The role of the solution in the process is simulated by specifying the probabilities (i.e., the rates) of molecular arrival. Thus a given saturation state is completely described by specifying the arrival rates of solution molecules at the solid surface. The reverse process is simulated by specifying the probabilities of molecule (adatom) departure from the surface (departure rates). This approach is capable of simultaneously treating a combination of dissolution and precipitation processes of a variety of different phases.

Several cement phases (both minerals and hydration products) are by their nature poorly constrained in terms of composition and crystallography, with the most obvious example being the calcium–silicate–hydrate (C–S–H) phase, but this does not necessarily limit the application of KMC techniques. Cement hydration may be in fact *the* original "many body problem": in other words, because cement hydration is not simply the sum of the hydration reactions for the individual phases, but depends on the *interaction* of these phases, the KMC approach provides a novel way of attacking this complex problem, provided data relating to the structure of the various reactant and product phases (C_3S, C_3A, C–S–H, ettringite, etc.) are available or can be calculated (see below).

An advantage of this approach is that the simulation can be adjusted for variations in the saturation state of the solution or the pH. Lasaga and Luttge [138] illustrated the case of an elementary reaction of bond-breaking and forming with the following example. They assumed that the total number of bonds between two A molecules (i.e., A–A bonds) on the dissolving surface is N_{AA}, and that the total number of broken A–A bonds on the same surface is N_{AA}^{broken}. Given that a steady state for these processes is achieved, this means that:

$$\frac{N_{AA}^{broken}}{N_{AA}} = \frac{k_-}{k_+} \tag{14}$$

where k_- and k_+ are the rate constants for the breaking and the formation of an A–A bond. If there are relatively few broken bonds at any one time, then $N_{AA} \sim N_{AA}^{tot} \sim$ constant. As a result, the probability that any one given A–A bond is broken is given by

$$P_{AA} = \frac{k_-}{k_+}. \tag{15}$$

Here, we ignore all other complexities in the process. Now, the rate of dissolution of molecules with n bonds depends only on: (i) the number of A molecules with n bonds on the surface, N_n^A, and (ii) the probability that all n bonds are indeed broken at the same time:

$$Dissolution\ Rate = (P_{AA})^n N_n^A. \tag{16}$$

Combining Eqs. (15) and (16) gives:

$$Rate = \left(\frac{k_-}{k_+}\right)^n N_n^A. \tag{17}$$

For cement systems a more comprehensive scenario might include additional complexities in the dissolution or growth process, for example the arrival of inhibitor or catalyst molecules at the surface and the surface diffusion of such adatoms. In the past, KMC simulations have been used successfully to analyze fundamental parameters and concepts such as activation energy, surface free energy, the solubility product, inhibition and catalysis, and the dependence on the saturation state of the solution (e.g., [132,155]). The crystal-based reaction mechanism used in these simulations has led to explanations for several experimental observations. It has also produced some unexpected results. For example, Lasaga and Luttge [139] observed the onset of reprecipitation of a secondary (amorphous) phase during the dissolution process of feldspar. This reaction was studied in more detail later by Zhang and Luttge [141], providing support for Hellmann's suggestion [156] that the so-called leached layer is in fact a re-precipitation product. This question was at the center of a controversial discussion for quite some time.

It should be noted that KMC models do not provide closed-form rate equations. Also, while other approaches generally seek to identify a rate-limiting step or process, such as the formation of a precursor complex [157], the KMC simulation derives mechanistic details that may lead to an improved fundamental understanding of the evolving system; i.e., no such *a priori* assumptions regarding reaction mechanisms are made. This stochastic approach fully incorporates the three-dimensional crystal lattice and investigates its interactions with an aqueous solution. While the model calculations do not require any assumptions about the reaction mechanism, a comprehensive parameterization is necessary. This means that beside crystallographic information about the lattice parameters, bond and eventually adsorption energies are required. If these data are not already published, they can be calculated in many cases by using *ab initio* and density functional theory (DFT) (e.g., [158]).

Today, *ab initio*/DFT modeling is a powerful method in itself. For example, it can be used to investigate the detailed reaction mechanism including the adsorption of H_2O, H^+, OH^- species due to pH variation, protonation and deprotonation processes, and the formation of possible reaction intermediates (e.g. [146,159–161]). It also allows the full reaction pathways of hydrolysis of surface Si–O–Si and Si–O–Al bonds, including the relevant transition states, to be investigated. However, in the context of KMC simulations it is mainly used for the parameterization of the MC model. The model results, once coupled with results from experimental measurements such as vertical scanning interferometry (VSI) and AFM (e.g., [145]), provide the ability to extract key kinetic properties such as changes in activation energy, catalytic and temperature effects, and the overall rate law. The combined results can then play an important role in eliminating hypotheses, focusing on new phenomena, and systematizing available experimental data. Overall, this approach could play

an important role in studying the complex kinetics of cement hydration, particularly at early ages.

5. Future contributions from hydration modeling and simulation

As the sophistication, power, and flexibility of hydration models and simulations continue to increase, improved experimental methods for characterizing materials structure, chemistry and surface phenomena are providing more detailed and accurate input data. The result is that computer models are becoming increasingly useful aides to conducting research into the fundamental mechanisms of hydration. Below is a representative list of outstanding issues, by no means comprehensive, for which the use of hydration models and simulations should prove useful. In all cases the use of models must be in conjunction with experiments.

5.1. The cause of the induction period

After decades of cement chemistry research, the basic mechanisms that cause the initiation and termination of the induction period of portland cement hydration remain arguably the most significant unanswered question regarding the hydration process. In recent years, a clearer picture is beginning to emerge as a result of combining experimental research and computer simulations (see the companion review on early-age mechanisms for a fuller discussion [1]). Settling this debate would have important implications for rationally designing chemical admixtures that can tailor the setting time and early-age properties of concrete. This question has been difficult to resolve because the controlling factors reside at the nanoscale, often at or near the surface of clinker minerals in the aqueous pore solution. Simulation models like HydratiCA have been used to test the plausibility of different mechanistic hypotheses, but they must be given information about the proposed mechanism to do so (i.e. the mechanism is an input rather than an output of such models). Fortunately, atomistic simulations have now reached a stage of sophistication where they are being used to complement recent advances in instrumentation for experimentally observing these nanoscale surface phenomena under realistic conditions. Through these combined computational and experimental methods, the mechanism(s) controlling the induction period may finally be determined unequivocally. Moreover, these same techniques can be used to extract molecular-scale nucleation and reaction rate data that can be upscaled to simulations like those discussed in Section 3.

5.2. Decelerating hydration rate and the size of the early rate peak

It is now well established that the early, acceleratory period of hydration leading up to the rate peak is controlled by the rate of nucleation and growth. However, this process cannot explain well the very slow and declining hydration rate that is often observed for weeks and even months after initial mixing, so it seems safe to assume that at least one shift in rate control occurs during the hydration process. It is commonly assumed that hydration eventually becomes diffusion controlled—that is, the rate of hydration is controlled by the rate at which the reactants can diffuse through the nanoporous layer of hydration product around the remaining unhydrated cement particles. However, space restrictions and the lack of availability of water can also restrict the hydration rate at later times. The point in the hydration process at which the rate controlling mechanism shifts away from nucleation and growth is not well established, and this is clearly an important aspect of the hydration process.

An early school of thought maintained that diffusion control was the cause of the main hydration peak; in other words, that the rapid deceleration following the peak results from the increasing amount of time required for reactants to diffuse through the product layer as it thickens. However, as discussed in Section 2.2, nucleation and growth modeling shows that this is not necessarily the case, as a peak rate followed by a deceleration period is a natural consequence of a nucleation and growth transformation, and in fact the boundary nucleation and growth model can fit most of the C_3S hydration peak quite well. Therefore, another school of thought holds that nucleation and growth control the entire early hydration period encompassed by the main rate peak, and that other mechanisms such as water consumption or diffusion only become rate controlling at later times when the rate has dropped to a small fraction of its peak value.

At present, neither hypothesis seems able to explain all of the experimental observations without proposing some modifications to the generally accepted picture of the hydration process. For example, nucleation and growth rate control appears to require that the hydration product forms initially with a much lower bulk density than was previously thought (see Sections 3.1 and 3.3). This is an important issue that can be resolved by a combination of modeling and experiments. In particular, boundary nucleation and growth models, incorporated into microstructural modeling platforms such as μic, have the potential to test a variety of scenarios on different systems. In particular, it appears that additives such as calcium chloride play an important role.

5.3. The role of sulfate in controlling early hydration of ordinary portland cement

Since the seminal study by Tenoutasse in 1968 [162] it has been recognized that C_3S hydration is strongly retarded in portland cements when the sulfate content is insufficient to promote complete conversion of C_3A to ettringite. Likewise, the presence of calcium sulfate in solution is known to mildly retard the hydration of pure C_3S, while calcium chloride is strongly accelerating [163]. However, a convincing mechanistic explanation for these admixture effects has not been given. Indeed, these admixture effects seem unusual at first because neither sulfate species nor chloride species participate in the reactions for simple C_3S dissolution or growth of C–S–H or CH. A key to understanding these admixture effects may be to understand whether selective adsorption of ions occurs at reactive surface sites of clinker minerals or hydration products. Recently, advanced techniques for probing nanoscale surface structure in controlled aqueous environments have been used in combination with Kinetic Monte Carlo simulations to elucidate the atomistic mechanisms of fluorite dissolution and exactly how different solution species can influence the rate [164]. Application of these same techniques to study the dissolution of clinker minerals in different solution environments will likely yield important insights about how admixtures can affect hydration rates especially at early ages.

5.4. Hydration of blended cements containing supplementary cementitious materials

The increasing use of supplementary cementitious materials (SCMs), also known as mineral admixtures, has further complicated the challenge of modeling the hydration kinetics of cements. SCMs are known to affect the hydration of cements in a variety of ways depending on their chemical composition, particle size distribution, and other factors. Many supplementary materials such as slag and fly ash are hydraulically active, meaning that they hydrate to form hydration products similar to portland cement. They also contribute to secondary pozzolanic reactions that consume calcium hydroxide formed by the portland cement hydration. These reactions occur at a much slower rate than the early hydration of the cement itself, and thus do not greatly contribute to the early hydration kinetics. However, by providing an active surface for nucleation of hydration product, SCMs can actually accelerate the early hydration of the cement itself. A likely scenario is that a small amount of early hydration creates C–S–H on the surface of the SCMs which acts as a

nucleation seed for further growth of hydration product [165]. SCMs can also affect the hydration process in other subtle ways. For example, because they react slowly, they effectively increase the amount of water available for hydration of the more reactive portland cement.

All of the above processes must be accounted for to successfully simulate the hydration of blended cements. This will likely require the application of more than one of the modeling platforms presented above. Given that the chemical behavior of SCMs can be extremely variable depending on their composition and that of the cement they are mixed with, their chemical actions could probably best be modeled on platforms that explicitly model the basic physical phenomena, such as HydratiCA. To simulate the hydration of a blended cement accurately, including particle size effects, the resulting data could be then be imported into a microstructure simulation platform such as μic.

6. General discussion—progress toward advanced hydration simulations

The last four decades of effort have resulted in significant advances in simulating the development of structure in cementitious materials at different length scales, and in modeling their hydration kinetics. This progress has happened in part by focusing on the underlying chemical and physical processes of hydration, including dissolution, nucleation and growth, and diffusion, as well as the evolution of pore structure and phase assemblages. With continued progress along these lines, it can be anticipated that simulation methods will become sophisticated enough that the hydration kinetics need not be modeled separately, but would be reproduced as a natural consequence of the hydration process.

Whereas a decade ago the goal may have been to perform such a complete simulation using a single modeling platform, recent developments discussed in this paper make it clear that this is unrealistic due to the complexity of the hydration process. A more likely scenario is that simulations performed at one length scale will provide input for independent simulations at the next (longer) length scale. In this case, the transfer of the results from one type of simulation to another is as important a step as the simulations themselves. This type of approach has already proven effective for predicting mechanical properties of cement paste and concrete: the bulk properties can be predicted by upscaling nanostructure-level models of the hydrated structure using multiscale poromechanics and granular mechanics approaches (see review in [166]).

The potential benefits of advanced hydration simulations are wide ranging. From a research point of view, simulations provide feedback for testing various hypotheses regarding the hydration mechanisms and exploring the effects of various chemical additives. For simulations based on fundamental, rather than empirical, models, there would also be the important capability of extension to novel cements with a variety of starting compositions. This would, for example, streamline the process of designing and verifying new, greener, cement-based materials.

From an engineering point of view, advanced hydration simulations would allow bulk properties, such as compressive strength and fluid permeability, to be calculated accurately from the starting composition. In terms of implementation, an advanced engineering simulation might take as its input the desired engineering properties of the concrete and the expected environmental conditions in the field and then, after accessing an extensive database of available cementitious materials and admixtures, and performing a series of comprehensive simulations, output detailed suggestions for materials selection, mixture proportioning, and processing such a concrete [166]. The realization of this type of simulation, or suite of simulations, is some distance in the future. However, many obstacles, such as lack of sufficient computing power, have receded during the past decade. Instead, the greatest obstacle to developing such fundamental and powerful simulations is presently a lack of understanding of fundamental mechanistic issues related to the hydration process. Both this paper and a companion paper [1] have described some of the most critical gaps in understanding. A sustained push to better understand the mechanisms underlying hydration with the use of new technologies and a synergy between numerical and experimental studies is needed in order to make the prediction of properties possible.

Acknowledgements

This paper is an outcome of the International Summit on Cement Hydration Kinetics and Modeling. The authors acknowledge financial support from the National Science Foundation (NSF) through Grant Award Nos. OISE-0757284 and CMS-0510854, the Federal Highway Administration (FHWA), Mapei, W. R. Grace, BASF, the Tennessee Technological University (TTU) Center for Manufacturing Research (CMR), the Canadian Research Center on Concrete Infrastructure (CRIB) and the Natural Science and Engineering Research Council of Canada (NSERCC). The authors would also like to acknowledge the organizers of the Summit including Joseph J. Biernacki (TTU), Will Hansen (University of Michigan), Jeffrey Bullard (National Institute of Standards and Technology) and Jacques Marchand (Laval University).

References

[1] J.W. Bullard, H.M. Jennings, R.A. Livingston, A. Nonat, G.W. Scherer, J.S. Schweitzer, K.S. Scrivener, J.J. Thomas, Mechanisms of cement hydration, Cement Concr. Res. 41 (2011) 1208–1223.
[2] R. Aris, Mathematical Modeling Techniques, Pitman, London, 1978.
[3] E.J. Garboczi, D.P. Bentz, Fundamental Computer Simulation Models for Cement-based Materials, in: J. Skalny, S. Mindess (Eds.), Materials Science of Concrete II, American Ceramic Society, Westerville, OH, 1991, pp. 249–273.
[4] T. Xie and J.J. Biernacki. The origins and evolution of cement hydration models. Comp. Concr. (in press).
[5] R. Kondo, S. Ueda, Kinetics and Mechanisms of the Hydration of Cements, Proceedings of the Fifth International Symposium on the Chemistry of Cement, Tokyo, 1968, pp. 203–248.
[6] R. Kondo, M. Kodama, On the hydration kinetics of cement, Semento Gijutsu Nenpo 21 (1967) 77–82. (in Japanese).
[7] J.M. Pommersheim, J.R. Clifton, Mathematical modeling of tricalcium silicate hydration, Cem. Concr. Res. 9 (1979) 765–770.
[8] J.M. Pommersheim, J.R. Clifton, G. Frohnsdorff, Mathematical modeling of tricalcium silicate hydration. II. Hydration sub-models and the effect of model parameters, Cem. Concr. Res. 12 (1982) 765–772.
[9] R.B. Williamson, Solidification of portland cement, Prog. Mater. Sci. 15 (1972) 189–286.
[10] H.M. Jennings and S.K. Johnson. Simulation of microstructure development during the hydration of a cement compound. J. Am. Ceram. Soc. 69 (1986) 790–795.
[11] J.H. Taplin, On the Hydration Kinetics of Hydraulic Cements, Proceedings of the 5th International Symposium on Chemistry of Cement, Tokyo, 1968, pp. 337–348.
[12] P.W. Brown, Effects of particle size distribution on the kinetics of hydration of tricalcium silicate, J. Am. Ceram. Soc. 72 (1989) 1829–1832.
[13] A. Bezjak, I. Jelenic, On the determination of rate constants for hydration processes in cement pastes, Cem. Concr. Res. 10 (1980) 553–563.
[14] A. Bezjak, Kinetic analysis of cement hydration including various mechanistic concepts. I. Theoretical development, Cem. Concr. Res. 13 (1983) 305–318.
[15] T. Knudsen, The dispersion model for hydration of Portland cement. 1. General concepts, Cem. Concr. Res. 14 (1984) 622–630.
[16] A. Bezjak, An extension of the dispersion model for the hydration of Portland cement, Cem. Concr. Res. 16 (1986) 260–264.
[17] A. Bezjak, Nuclei growth model in kinetic analysis of cement hydration, Cem. Concr. Res. 16 (1986) 605–609.
[18] L.J. Parrot, D.C. Killoh, Prediction of cement hydration, Br. Ceram. Proc. 35 (1984) 41–53.
[19] F. Tomosawa, Development of a Kinetic Model for Hydration of Cement, in: H. Justnes (Ed.), Proceedings of the Tenth International Congress on the Chemistry of Cement, Göteburg, Sweden, 1997, p. 2ii051.
[20] B. Lothenbach, F. Winnefeld, Thermodynamic modelling of the hydration of portland cement, Cem. Concr. Res. 36 (2006) 209–226.
[21] E. Guillon, J.J. Chen, G. Chanvillard, Physical and Chemical Modeling of the Hydration Kinetics of OPC Paste Using a Semi-analytical Approach, in: E. Schlangen, G. de Schutter (Eds.), Proceedings of ConMod'08: International RILEM Symposium on Concrete Modelling, Delft, The Netherlands, 2008, pp. 165–172.
[22] J.W. Bullard, B. Lothenbach, P.E. Stutzman, K.A. Snyder, Coupling thermodynamics and digital image models to simulate hydration and microstructure development of portland cement paste, J. Mater. Res. 26 (2011) 609–622.

[23] S. Garrault-Gauffinet, A. Nonat, Experimental investigation of calcium silicate hydrate (C–S–H) nucleation, J. Cryst. Growth 200 (1999) 565–574.
[24] S. Garrault, A. Nonat, Hydrated layer formation on tricalcium and dicalcium silicate surfaces: experimental study and numerical simulations, Langmuir 17 (2001) 8131–8138.
[25] J.W. Christian, The Theory of Transformations in Metals and Alloys, Part 1, 3rd edition. Pergamon Press, Oxford, 2002.
[26] M. Avrami. Kinetics of Phase Change. J. Chem. Phys., 7, 1103–1112 (1939) and 1108, pp. 1212–1124 (1940).
[27] P.W. Brown, J.M. Pommersheim, G. Frohnsdorff, A kinetic model for the hydration of tricalcium silicate, Cem. Concr. Res. 15 (1985) 35–41.
[28] W.A. Johnson, R.F. Mehl, Reaction kinetics in processes of nucleation and growth, Trans. Am. Inst. Min. Metall. Eng. 135 (1939) 416.
[29] A.N. Kolmogorov, A statistical theory for the recrystallization of metals, Bull. Acad. Sci. USSR Phys. Ser 1 (1937) 255.
[30] N. Tenoutasse, A. de Donder, The kinetics and mechanism of hydration of tricalcium silicate, Silicates Ind. 35 (1970) 301–307.
[31] R. Kondo, M. Daimon, Early hydration of tricalcium silicate: a solid reaction with induction and acceleration periods, J. Am. Ceram. Soc. 52 (1969) 503–508.
[32] A. Damasceni, L. Dei, E. Fratini, F. Ridi, S.H. Chen, P. Baglioni, A novel approach based on differential scanning calorimetry applied to the study of tricalcium silicate hydration kinetics, J. Phys. Chem. B 106 (2002) 11572–11578.
[33] F. Ridi, L. Dei, E. Fratini, S.-H. Chen, P. Baglioni, Hydration kinetics of tri-calcium silicate in the presence of superplasticizers, J. Phys. Chem. B 107 (2003) 1056–1061.
[34] G.W. Scherer, Freezing gels, J. Non-Cryst. Solids 155 (1993) 1–25.
[35] D.D. Double, A. Hellawell, S.J. Perry, The hydration of Portland cement, Proc. R. Soc. London Ser. A 359 (1978) 435–451.
[36] J.J. Thomas, H.M. Jennings, Effects of D_2O and mixing on the early hydration kinetics of tricalcium silicate, Chem. Mater. 11 (1999) 1907–1914.
[37] R. Berliner, M. Popvici, K.W. Herwig, M. Berliner, H.M. Jennings, J.J. Thomas, Quasielastic neutron scattering study of the effect of water to cement ratio on the hydration kinetics of tricalcium silicate, Cem. Concr. Res. 28 (1998) 231–243.
[38] S.A. FitzGerald, D.A. Neumann, J.J. Rush, D.P. Bentz, R.A. Livingston, In-situ quasielastic neutron scattering study of the hydration of tricalcium silicate, Chem. Mater. 10 (1998) 397–402.
[39] A.J. Allen, J.C. McLaughlin, D.A. Neumann, R.A. Livingston, In situ quasi-elastic scattering characterization of particle size effects on the hydration of tricalcium silicate, J. Mater. Res. 19 (2004) 3242–3254.
[40] D.R. Vollet, A.F. Craievich, Effects of temperature and of the addition of accelerating and retarding agents on the kinetics of hydration of tricalcium silicate, J. Phys. Chem. B 104 (2000) 12143–12148.
[41] E.M. Gartner, J.M. Gaidis, Hydration Mechanisms, I, in: J.P. Skalny (Ed.), Materials Science of Concrete, The American Ceramic Society, Westerville, OH, 1989, pp. 95–125.
[42] V.K. Peterson, D.A. Neumann, R.A. Livingston, Hydration of tricalcium and dicalcium silicate mixtures studied using quasielastic neutron scattering, J. Phys. Chem. B 109 (2005) 14449–14453.
[43] V.K. Peterson, D.A. Neumann, R.A. Livingston, Hydration of cement: the application of quasielastic and inelastic neutron scattering, Phys. B Condensed Matter 385 (2006) 481–486.
[44] V.K. Peterson, M.C.G. Juenger, Hydration of tricalcium silicate: effects of $CaCl_2$ and sucrose on reaction kinetics and product formation, Chem. Mater. 18 (2006) 5798–5804.
[45] E.M. Gartner, J.F. Young, D.A. Damidot, I. Jawed, Hydration of Portland Cement, in: P. Barnes, J. Bensted (Eds.), Chapter 3 in Structure and Performance of Cements, 2nd ed., Spon Press, London, 2002, pp. 57–113.
[46] J.J. Thomas, A new approach to modeling the nucleation and growth kinetics of tricalcium silicate hydration, J. Am. Ceram. Soc. 90 (2007) 3282–3288.
[47] S. Garrault, A. Nonat, Hydrated layer formation on tricalcium and dicalcium silicate surfaces: experimental study and numerical simulations, Langmuir 17 (2001) 8131–8138.
[48] J.W. Cahn, The kinetics of grain boundary nucleated reactions, Acta Metall. 4 (1956) 449–459.
[49] V.K. Peterson, A.E. Whitten, Hydration processes in tricalcium silicate: application of the boundary nucleation model to quasielastic neutron scattering data, J. Phys. Chem. C 113 (2009) 2347–2351.
[50] J.J. Thomas, A.J. Allen, H.M. Jennings, Hydration kinetics and microstructure development of normal and $CaCl_2$-accelerated tricalcium silicate (C_3S) pastes, J. Phys. Chem. C 113 (2009) 19836–19844.
[51] G.W. Scherer, G.P. Funkhouser, S. Peethamparan, Effect of pressure on early hydration of Class H and white cement, Cem. Concr. Res. 40 (2010) 845–850.
[52] J.W. Bullard, A determination of hydration mechanisms for tricalcium silicate using a kinetic cellular automaton model, J. Am. Ceram. Soc. 91 (2008) 2088–2097.
[53] G.W. Scherer, J. Zhang, and J.J. Thomas. Nucleation and growth models for hydration of cement (in preparation).
[54] J.W. Cahn, The time cone method for nucleation and growth kinetics on a finite domain, Mater. Res. Soc. Symp. Proc. 398 (1996) 425–437.
[55] E. Villa, P.R. Rios, Transformation kinetics for surface and bulk nucleation, Acta Mater. 58 (2010) 2752–2768.
[56] G.J.C. Frohnsdorff, W.G. Freyer, P.D. Johnson, The Mathematical Simulation of Chemical, Physical and Mechanical Changes Accompanying the Hydration of Cement, 5th Int. Congr. Chem. Cem., Tokyo, 2, 1968, p. 321.
[57] H.M. Jennings, S.K. Johnson, Simulation of microstructure development during the hydration of a cement compound, J. Am. Ceram. Soc. 69 (1986) 790–795.
[58] P. Meakin, Off lattice simulations of cluster–cluster aggregateion in dimensions 2–6, Phys. Lett. A 107 (1985) 269–272.
[59] S. Bishnoi, K.L. Scrivener, μic: a new platform for modelling the hydration of cements, Cem. Concr. Res. 39 (2009) 266–274.
[60] K. van Breugel, Numerical simulation of hydration and microstructural development in hardening cement paste (I): theory, Cem. Concr. Res. 25 (1995) 319–331.
[61] D.P. Bentz, Three-dimensional computer simulation of cement hydration and microstructure development, J. Am. Ceram. Soc. 80 (1997) 3–21.
[62] K. van Breugel, Numerical simulation of hydration and microstructural development in hardening cement paste (II): applications, Cem. Concr. Res. 25 (1995) 522–530.
[63] E.A.B. Koenders, K. van Breugel, Numerical modelling of autogeneous shrinkage of hardening cement paste, Cem. Concr. Res. 27 (1997) 1489–1499.
[64] G. Ye, K. van Breugel, A.L.A. Fraaij, Three-dimensional microstructure analysis of numerically simulated cementitious materials, Cem. Concr. Res. 33 (2003) 215–222.
[65] D.P. Bentz, E.J. Garboczi, A digitized simulation model for microstructural development, Ceram. Trans. 16 (1991) 211–226.
[66] E.J. Garboczi, D.P. Bentz, Computer simulation of the diffusivity of cement-based materials, J. Mater. Sci. 27 (1992) 2083–2092.
[67] D.P. Bentz, CEMHYD3D: A Three-dimensional Cement Hydration and Microstructure Development Modeling Package. Version 3.0, NISTIR 7232, U.S. Department of Commerce, 2005, Available at, http://concrete.nist.gov/monograph.
[68] J.W. Bullard, E.J. Garboczi, A model investigation of the influence of particle shape on Portland cement hydration, Cem. Concr. Res. 36 (2006) 1007–1015.
[69] E.J. Garboczi, J.W. Bullard, Shape analysis of a reference cement, Cem. Concr. Res. 34 (2004) 1933–1937.
[70] D.P. Bentz, Quantitative comparison of real and CEMHYD3D simulated cement paste microstructures, Cem. Concr. Res. 34 (2004) 3–7.
[71] D.P. Bentz, O.M. Jensen, A.M. Coats, F.P. Glasser, Influence of silica fume on diffusivity in cement-based materials I. Experimental and computer modeling studies on cement pastes, Cem. Concr. Res. 30 (2000) 953–962.
[72] J.M. Torrents, T.O. Mason, E.J. Garboczi, Impedance spectra of fiber-reinforced cement-based composites: a modeling approach, Cem. Concr. Res. 30 (2000) 585–592.
[73] K.A. Snyder, J.W. Bullard, Effect of Continued Hydration on the Transport Properties of Cracks through Portland Cement Pastes in a Saturated Environment: A Microstructural Model Study, NIST IR 7265, U.S. Department of Commerce, Washington, DC, 2005.
[74] C.J. Haecker, E.J. Garboczi, J.W. Bullard, R.B. Bohn, Z. Sun, S.P. Shah, T. Voigt, Modeling the linear elastic properties of Portland cement paste, Cem. Concr. Res. 35 (2005) 1948–1960.
[75] D.P. Bentz, An argument for using coarse cements in high performance concretes, Cem. Concr. Res. 29 (1999) 615–618.
[76] D.P. Bentz, E.J. Garboczi, C.J. Haecker, O.M. Jensen, Effects of cement particle size distribution on performance properties of cement-based materials, Cem. Concr. Res. 29 (1999) 1663–1671.
[77] D.P. Bentz, O.M. Jensen, K.K. Hansen, J.F. Oleson, H. Stang, C.J. Haecker, Influence of cement particle size distribution on early age autogenous strains and stresses in cement-based materials, J. Am. Ceram. Soc. 84 (2000) 129–135.
[78] E.J. Garboczi, D.P. Bentz, The effect of statistical fluctuation, finite size error, and digital resolution on the phase percolation and transport properties of the NIST cement hydration model, Cem. Concr. Res. 31 (2001) 1501–1514.
[79] J.W. Bullard, Approximate rate constants for nonideal diffusion and their application in a stochastic model, J. Phys. Chem. A 111 (2007) 2084–2092.
[80] J.W. Bullard, A three-dimensional microstructural model of reactions and transport in aqueous mineral systems, Modell. Simul. Mater. Sci. Eng. 15 (2007) 711–738.
[81] T. Karapiperis, B. Blankleider, Cellular automaton model of reaction-transport processes, Physica D 78 (1994) 30–64.
[82] J.W. Bullard, R.J. Flatt, New insights into the effect of calcium hydroxide precipitation on the kinetics of tricalcium silicate hydration, J. Am. Ceram. Soc. 93 (2010) 1894–1903.
[83] P. Navi, C. Pignat, Simulation of cement hydration and the connectivity of the capillary pore space, Adv. Cem. Based Mater. 4 (1996) 58–67.
[84] S. Bishnoi, K.L. Scrivener, Studying nucleation and growth kinetics of alite hydration using μic, Cem. Concr. Res. 39 (2009) 849–860.
[85] I.K. Karpov, K.V. Chudnenko, D.A. Kulik, Modeling chemical mass-transfer in geochemical processes: thermodynamic relations, conditions of equilibria and numerical algorithms, Am. J. Sci. 297 (1997) 767–806.
[86] B. Lothenbach, F. Winnefeld, Thermodynamic modelling of the hydration of Portland cement, Cement Concr. Res. 36 (2006) 209–226.
[87] S. Garrault, E. Finot, E. Lesniewska, A. Nonat, Study of C–S–H growth on C_3S surface during its early hydration, Mater. Struct. 38 (2005) 435–442.
[88] J. Zhang, E.A. Weissinger, S. Peethamparan, G.W. Scherer, Early hydration and setting of oil well cement, Cem. Concr. Res. 40 (2010) 1023–1033.
[89] A.C. Lasaga, A. Luttge, Variation of crystal dissolution rate based on a dissolution step wave model, Science 291 (2001) 2400–2404.
[90] P.M. Dove, N. Han, J.J. De Yoreo, Mechanisms of classical crystal growth theory explain quartz and silicate dissolution behavior, Proc. Natl. Acad. Sci. 102 (2005) 15357–15362.
[91] P. Juilland, E. Gallucci, R. Flatt, K. Scrivener, Dissolution theory applied to the induction period in alite hydration, Cem. Concr. Res. 40 (2010) 831–844.
[92] J.F. Young, H.S. Tong, R.L. Berger, Compositions of solutions in contact with hydrating tricalcium silicate pastes, J. Am. Ceram. Soc. 60 (1977) 193–198.

[93] I. Jawed, J. Skalny, Surface phenomena during tricalcium silicate hydration, J. Colloid Interface Sci. 85 (1982) 235–243.
[94] J.W. Bullard, E. Enjolras, W.L. George, S.G. Satterfield, J.E. Terrill, A parallel reaction-transport model applied to cement hydration and microstructure development, Model. Simul. Mater. Sci. Eng. 15 (2010) 711–738.
[95] A. Bezjak, I. Jelenic, On the determination of rate constants for hydration processes in cement pastes, Cem. Concr. Res. 10 (1980) 553–563.
[96] M. Costoya, "Kinetics and microstructural investigation on the hydration of tricalcium silicate", Doctoral Thesis, École Polytechnique Fédérale de Lausanne, Switzerland (2008).
[97] H.M. Jennings, A model for the microstructure of calcium silicate hydrate in cement paste, Cem. Concr. Res. 30 (2000) 101–116.
[98] A.J. Allen, J.J. Thomas, H.M. Jennings, Composition and density of nanoscale calcium–silicate–hydrate in cement, Nat. Mater. 6 (2007) 311–316.
[99] P. Hohenberg, W. Kohn, Inhomogeneous electron gas, Phys. Rev. B 36 (1964) 864–871.
[100] W. Kohn, L.J. Sham, Self-consistent equations including exchange and correlation effects, Phys. Rev. A140 (1965) 1133–1138.
[101] J.B. Foresman, A. Frisch, Exploring Chemistry with Electronic Structure Methods, Second EditionGaussian Inc., Pittsburgh, PA, 1996.
[102] A.R. Leach, Molecular Modelling: Principles and Applications, 2nd Ed. Prentice-Hall, 2001.
[103] R. Car, M. Parrinello, Unified approach for molecular dynamics and density-functional theory, Phys. Rev. Lett. 55 (1985) 2471–2474.
[104] G. Henkelmann, H. Jonsson, Long time scale kinetic Monte Carlo simulations without lattice approximation and predefined event table, J. Chem. Phys. 115 (21) (2001) 9657–9666.
[105] A.F. Voter, F. Montalenti, T.C. Germann, Extending the time-scale in atomistic simulations of materials, Annu. Rev. Mater. Res. 32 (2002) 321–346.
[106] K.L. Scrivener, R.J. Kirkpatrick, Innovation in use and research on cementitious material, Cem. Concr. Res. 38 (2008) 128–136.
[107] G.W. Scherer, Structure and properties of gels, Cem. Concr. Res. 29 (1999) 1149–1157.
[108] J.J. Thomas, H.M. Jennings, A colloidal interpretation of chemical aging of the C–S–H gel and its effects on the properties of cement paste, Cem. Concr. Res. 36 (2006) 30–38.
[109] S.V. Churakov, Hydrogen bond connectivity in jennite from *ab initio* simulations, Cem. Concr. Res. 38 (2008) 1359–1364.
[110] E. Bonaccorsi, S. Merlino, H.F.W. Taylor, The crystal structure of jennite, $Ca_9Si_6O_{18}(OH)_6\cdot 8H_2O$, Cem. Concr. Res. 34 (2004) 1481–1488.
[111] S.V. Churakov, Structure of the interlayer in normal 11 angstrom tobermorite from an *ab initio* study, Eur. J. Mineralog. 21 (2009) 261–271.
[112] S.V. Churakov, Structural position of H_2O molecules and hydrogen bonding in anomalous 11 angstrom tobermorite, Am. Mineralog. 94 (2009) 156–165.
[113] A. Gmira, M. Zabat, R.J.-M. Pellenq, H. Van Damme, Microscopic physical basis of the macroscopic poromechanical behavior of concrete, Mater. Struct. Concr. Sci. Eng. 37 (2004) 3–14.
[114] R.J.-M. Pellenq, N. Lequeux, H. van Damme, Engineering the bonding scheme in C–S–H: the iono-covalent framework, Cem. Concr. Res. 38 (2008) 159–174.
[115] S.A. Hamid, The crystal structure of the 11A natural tobermorite $Ca_{2.25}[Si_3O_{7.5}(OH)_{1.5}].1\ H_2O$, Z. Kristallogr. 154 (1981) 189–198.
[116] S. Merlino, E. Bonaccorsi, T. Armbruster, The real structure of tobermorite 11 angstrom: normal and anomalous forms, OD character and polytypic modifications, Eur. J. Mineralog. 13 (2001) 577–590.
[117] H. Manzano. Atomistic simulation studies of the cement paste components, Thesis; University of the Basque Country UPV/EHU (2009).
[118] G. Constantinides, F.-J. Ulm, The nanogranular nature of C–S–H, J. Mech. Phys. Solids 55 (2007) 64–90.
[119] H. Manzano, J.S. Dolado, A. Ayuela, Elastic properties of the main species present in Portland cement pastes, Acta Mater. 57 (2009) 1666–1674.
[120] R. Shahsavari, M.J. Buehler, R.J.-M. Pellenq, F.J. Ulm, First-principles study of elastic constants and interlayer interactions of complex hydrated oxides: case study of tobermorite and jennite, J. Am. Ceram. Soc. 92 (2009) 2323–2330.
[121] H. Manzano, A. Ayuela, J.S. Dolado, On the formation of cementitious C–S–H nanoparticles, J. Comput.-Aided Mater. Des. 14 (2007) 45–51.
[122] A. Delville, R.J.-M. Pellenq, Electrostatic attraction and/or repulsion between charged colloids: a (NVT) Monte-Carlo study, Mol. Simul. 24 (2000) 1–24.
[123] R.J.-M. Pellenq, J.M. Caillol, A. Delville, Electrostatic attraction between two charged surfaces: A (N, V, T) Monte Carlo simulation, J. Phys. Chem. B 101 (1997) 8584–8594.
[124] B. Jöhnson, A. Nonat, C. Labbez, B. Cabane, H. Wennerström, Controlling the cohesion of cement paste, Langmuir 21 (2005) 9211–9221.
[125] A. Ayuela, J.S. Dolado, I. Campillo, Y.R. de Miguel, E. Erkizia, D. Sanchez-Portal, A. Rubio, A. Porro, P.M. Echenique, Silicate chain formation in the nanostructure of cement-based materials, J. Chem. Phys. 127 (2007) 164710.
[126] H. Manzano, J.S. Dolado, A. Ayuela, Aluminum incorporation to dreierketten silicate chains, J. Phys. Chem. B 113 (2009) 2832–2839.
[127] J.S. Dolado, M. Griebel, J. Hamaekers, A molecular dynamics study of calcium silicate hydrate (C–S–H) gels, J. Am. Ceram. Soc. 90 (2007) 3938–3942.
[128] H. Manzano, J.S. Dolado, M. Griebel, J. Hamaekers, A molecular dynamics study of the aluminosilicate chains structure in Al-rich calcium silicate hydrated (C–S–H) gels, Phys. Status Solidi Appl. Mater. Sci. 205 (2008) 1324–1329.
[129] R.J.-M. Pellenq, A. Kushima, R. Shahsavari, K.J. Van Vliet, M.J. Buehler, S. Yip, F.J. Ulm, A realistic molecular model of cement hydrates, PNAS 106 (2009) 16102–16107.
[130] J.J. Thomas, H.M. Jennings, A.J. Allen, Relationships between composition and density of tobermorite, jennite, and nanoscale $CaO–SiO_2–H_2O$, J. Phys. Chem. C 114 (2010) 7594–7601.
[131] A. Luttge, Crystal Dissolution Kinetics Studied by Vertical Scanning Interferometry and Monte Carlo Simulations: A Brief Review and Outlook, in: X.-Y. Liu, J.J. De Yoreo (Eds.), Nanoscale Structure and Assembly at Solid–Fluid Interfaces. Vol. I. Interfacial Structures versus Dynamics. Series on Nanoscience and Technologies, Kluwer Academic Publisher, 2004, pp. 209–247.
[132] J. Cama, L. Zhang, G. de Giudici, J.M. Soler, R.S. Arvidson, A. Luttge, Dissolution of fluorite (111) cleavage surface in acid pH: VSI, AFM and Monte Carlo simulations, Geochim. Cosmochim. Acta 73:A (2009).
[133] Molecular Modeling Theory: Applications in the Geosciences, R.T. Cygan, J.D. Kubicki (Eds.), Reviews in Mineralogy & Geochemistry, 42, Mineralogical Society of America, Washington, DC, 2001.
[134] W.H. Casey, J.R. Rustad, L. Spiccia, Minerals as molecules—use of aqueous oxide and hydroxide, Eur. Chem. J. 15 (2009) 4496–4515.
[135] C.A. Ohlin, E.M. Villa, J.R. Rustad, W.H. Casey, Dissolution of insulating oxide materials at the molecular scale, Nat. Mater. 9 (2010) 11–19.
[136] A.C. Lasaga, A. Luttge, Variation of crystal dissolution rate based on a dissolution stepwave model, Science 291 (2001) 2400–2404.
[137] A.C. Lasaga, A. Luttge, A model for crystal dissolution, Eur. J. Mineralog. 15/4 (2003) 603–615.
[138] A.C. Lasaga, A. Luttge, Mineralogical approaches to fundamental crystal dissolution kinetics, Am. Mineralog. 89 (2004) 527–540.
[139] A.C. Lasaga, A. Luttge, Mineralogical approaches to fundamental crystal dissolution kinetics—dissolution of an A_3B structure, Eur. J. Mineralog. 16 (2004) 713–729.
[140] L. Zhang, A. Luttge, Computer simulations of Al, Si order in albite and its effect on albite dissolution processes: a Monte Carlo study, Am. Mineralog. 90 (2007) 1316–1324.
[141] L. Zhang, A. Luttge, Aluminosilicate dissolution kinetics: a general stochastic model, J. Phys. Chem. B 112 (2008) 1736–1742.
[142] L. Zhang, A. Luttge, Morphological evolution of dissolving feldspar particles with anisotropic surface kinetics and implications for dissolution rate normalization and grain size dependence: a kinetic modeling study, Geochim. Cosmochim. Acta 73 (2009) 6757–6770.
[143] P. Meakin, K.M. Rosso, Simple kinetic Monte Carlo models for dissolution pitting induced by crystal defects, J. Chem. Phys. 129 (2008) 204106.
[144] S.C. Parker, N.H. de Leeuw, E. Bourova, D.J. Cooke, Application of Lattice Dynamics and Molecular Dynamics Techniques to Minerals and their Surfaces, Molecular Modeling Theory: Applications in the Geosciences, in: R.T. Cygan, J.D. Kubicki (Eds.), Reviews in Mineralogy & Geochemistry, 42, Mineralogical Society of America, Washington, DC, 2001, pp. 63–82.
[145] A. Luttge and R.S. Arvidson, Processes, Kinetics and Material Properties: A New Approach Integrating Interferometry and Kinetic Simulations, J. Am. Ceram. Soc. 93 (2010) 3519–3530.
[146] A.C. Lasaga, G.V. Gibbs, *Ab initio* quantum mechanical calculations of water–rock interactions: adsorption and hydrolysis reactions, Am. J. Sci. 290 (1990) 263–295.
[147] A.C. Lasaga, Kinetic Theory in Earth Sciences, Princeton Series in Geochem. Princeton University Press, Princeton, N.J., 1998
[148] G.H. Gilmer, Computer models of crystal growth, Science 208 (1978) 355–363.
[149] G.H. Gilmer, Computer simulations of crystal growth, J. Cryst. Growth 42 (1977) 3–10.
[150] G.H. Gilmer, Growth on imperfect crystal faces. I. Monte Carlo growth rates, J. Cryst. Growth 35 (1976) 15–28.
[151] A.C. Lasaga, A.E. Blum, Surface chemistry, etch pits and mineral–water reactions, Geochim. Cosmochim. Acta 50 (1986) 2263–2279.
[152] A.E. Blum, A.C. Lasaga, Aquatic Surface Chemistry; Chemical Processes at the Particle–Water Interface, in: W. Stumm (Ed.), Environm. Sci. & Techn. Series, J. Wiley, New York, 1987, pp. 255–292.
[153] B. Wehrli, Monte-Carlo simulations of surface morphologies during mineral dissolution, J. Colloid Interface Sci. 132 (1989) 230–242.
[154] J.P. van der Eerden, P. Bennema, T.A. Cheiepanova, Survey of Monte Carlo simulations of crystal surfaces and crystal growth, Prog. Cryst. Growth Charact. 1 (1978) 219–251.
[155] A.C. Lasaga, A. Luttge, Kinetic justification of the solubility product: application of a general kinetic dissolution model, J. Chem. Phys. B 109 (2005) 1635–1642.
[156] R. Hellmann, J.-M. Penisson, R.L. Hervig, J.-H. Thomassin, M.-F. Abrioux, An EFTEM/HRTEM high-resolution study of the near surface of labradorite feldspar altered at acid pH: evidence for interfacial dissolution–reprecipitation, Phys. Chem. Min. 30 (2003) 192–197.
[157] E.H. Oelkers, General kinetic description of multioxide silicate mineral and glass dissolution, Geochim. Cosmochim. Acta 65 (2001) 3703–3720.
[158] Y. Xiao, A. Luttge, Solvated *Ab initio* and Density Functional Theory (DFT) Modeling of Mineral–Fluid Surface Reactions: Towards a Fundamental Understanding of Aluminosilicate Dissolution Mechanisms, 2002.
[159] A.C. Lasaga, Atomic treatment of mineral–water surface reactions, In Rev. Mineralog. 23 (1992) 17–80.
[160] Y. Xiao, A.C. Lasaga, *Ab initio* quantum mechanical studies of the kinetics and mechanisms of silicate dissolution: H_3O^+ catalysis, Geochim. Cosmochim. Acta 58 (1994) 5379–5400.
[161] Y. Xiao, A.C. Lasaga, *Ab initio* quantum mechanical studies of the kinetics and mechanisms of quartz dissolution: OH^- catalysis, Geochim. Cosmochim. Acta 60 (1996) 2283–2295.
[162] N. Tenoutasse, The Hydration Mechanism of C_3A and C_3S in the Presence of Calcium Chloride and Calcium Sulphate, Proceedings of the Fifth

International Symposium on the Chemistry of Cement, Tokyo, Japan, Vol. II, 1968, pp. 372–378.
[163] P.W. Brown, C.L. Harner, E.J. Prosen, The effect of inorganic salts on tricalcium silicate hydration, Cem. Concr. Res. 16 (1985) 17–22.
[164] J. Cama, L. Zhang, G. De Guidici, J.M. Soler, R.S. Arvidson, A. Luttge, Dissolution of fluorite (111) cleavage surface in acid pH: VSI, AFM, and Monte Carlo simulations, Geochim. Cosmochim. Acta 73 (2009) A187.
[165] J.J. Thomas, H.M. Jennings, J.J. Chen, Influence of nucleation seeding on the hydration mechanisms of tricalcium silicate and cement, J. Phys. Chem. C 113 (2009) 4327–4334.
[166] H.M. Jennings, J.W. Bullard, J.J. Thomas, J.E. Andrade, J.J. Chen, G.W. Scherer, Characterization and modeling of pores and surfaces in cement paste: correlations to processing and properties, J. Adv. Concr. Technol. 6 (2008) 5–29.